HYDROTHERMAL MODELING FOR OPTIMUM TEMPERATURE CONTROL: AN ESTIMATION-THEORETIC APPROACH

by

Bradley P. Schrader and Stephen F. Moore

Energy Laboratory Report No. MIT-EL 76-007

July 1976

HYDROTHERMAL MODELING FOR OPTIMUM TEMPERATURE CONTROL: AN ESTIMATION-THEORETIC APPROACH

by

Bradley P. Schrader

and

Stephen F. Moore

Energy Laboratory

and

Department of Civil Engineering

Massachusetts Institute of Technology
Cambridge, Massachusetts 02139

sponsored by
New England Power Company

under the

MIT Energy Laboratory Electric Power Program

Energy Laboratory Report No. MIT-EL 76-007

July 1976

HYDROTHERMAL MODELING FOR OPTIMUM TEMPERATURE CONTROL: AN ESTIMATION-THEORETIC APPROACH

ABSTRACT

A short-term temperature forecasting (STF) system is proposed to predict and control plant intake and discharge temperatures at Salem Harbor Electric Generating Station. It is desired to minimize receiving-water (i.e., intake-water) temperatures during peak power demand periods, in order to minimize the cost of complying with the maximum discharge water temperature limit. This study addresses the hydrothermal modeling requirements of an STF system.

An important element of an STF system is a predictive model of plant intake water temperatures. For application to Salem Harbor Station, strict model performance criteria exist, defining a model development problem: Develop a simple model to predict plant intake water temperatures 24 hours ahead, predicting daily peak intake temperatures within 1°F on 90% of the days, and using only existing measurements. An estimation-theoretic approach to model development is used, which quantifies and minimizes the uncertainties in the model. The approach employs optimal filtering and full-information maximum-likelihood (FIML) estimation to obtain optimum parameter estimates. A two-basin, two-layer hydrothermal model of Salem Harbor is developed. The model computes hourly intake temperatures, incorporating tidal flushing, stratification, surface heat exchange, and wind advection of the plume. Twenty-eight model parameters and five noise statistics are estimated from intake temperature data.

Preliminary best-fit parameter values are obtained subjectively, followed by FIML parameter estimation using a data base of 96 hourly measurements (7/29 - 8/2/74). The model is tested for 106 days (5/17-9/20/74) and various performance measures are computed, including sum-of-squares of measurement residuals (S), whiteness (P), percent of daily peak temperature predictions within 1°F of actual (T), and others. Visual inspection of 24-hour intake temperature predictions shows that the two-basin, two-layer model performs qualitatively well. However, the model fails statistical tests on S and P, indicating structural weaknesses. FIML estimation yields physically unrealistic values for certain parameters, probably compensating for inadequate model structure. Despite structural flaws in the two-basin, two-layer model, FIML estimation yields parameters with consistently better performance than the preliminary estimates (by a small amount).

It is concluded that the two-basin, two-layer model is presently unsuitable for STF use, largely due to structural weaknesses. Possible corrections are suggested; however, a statistical model of hourly temperatures appears to offer greater potential accuracy than physically-derived models. FIML parameter estimation is shown to be useful for water quality model development on a real system, particularly after subjective model development has been exhausted.

ACKNOWLEDGEMENTS

Several M.I.T. associates assisted us in this work: Dr. David. W. Peterson provided practical advice and perceptive guidance on the use of estimation methods. Mr. Christopher Eckel skillfully assisted the computational efforts. Dr. Gerhard Jirka and Professor Keith Stolzenbach assisted with their experience in hydrothermal modeling.

Mr. A. Rayner Kenison, of the New England Power Company, provided useful guidance from the client's perspective. Providing helpful assistance were Messers. Philip D. Domenico, Kenneth Galli, and Robert McMonagle.

Thanks are due to Mrs. Jean Coleman for her untiring efforts in typing this report. A-Plus Secretarial Services provided skilled and timely assistance.

This report represents a portion of Mr. Schrader's thesis, submitted for the Degree Environmental Engineer: "Once-Through Cooling at Salem Harbor Electric Generating Station: Short-term Temperature Forecasting, and Policy Aspects of a Temperature Standard". Policy aspects of the thesis are not included herein.

This research was supported by the New England Power Company, through the M.I.T. Energy Laboratory, Electric Power Program. Their support is gratefully acknowledged. All computation was done at the M.I..T. information Processing Center. Graphics were done by M.I.T. Graphic Arts.

TABLE OF CONTENTS

LIST OF TABLES

LIST OF FIGURES

CHAPTER ONE

INTRODUCTION

1.1 Background

The focus of this study is a proposed computerized system for short-term forecasting and control of discharge temperatures at Salem Harbor Electric Generating Station. Salem Harbor Station is a 750 megawatt steam-electric generating station located in Salem, Massachusetts, on the Atlantic Coast just north of Boston (see Figure 1-1). The New England Power Company (NEPCO) owns and operates the fossil-fueled station. The plant employs a once-through condenser-cooling system, withdrawing seawater from Salem Harbor, and discharging the heated water back into the Harbor (see Figure 1-2). When the temperature of this discharged water threatens to exceed the State maximum discharge temperature limitation (T_{max}), the plant must reduce power production to reduce the heat added to the discharge. These unscheduled load reductions force the station to purchase make-up power, frequently at peak prices (during peak demand periods).

The objective of the proposed short-term temperature forecasting (STF) system is to reduce the cost of compliance with the present discharge limitation. Hourly electric power generation is economically scheduled, taking into account the heat retention capacity of Salem Harbor, the difference in wholesale electric power costs between day and night, and the maximum discharge temperature limitation. The system is based on the assumption that a fraction of discharged heat re-enters the cooling system (6 to 12 hours later), as warmer-than-

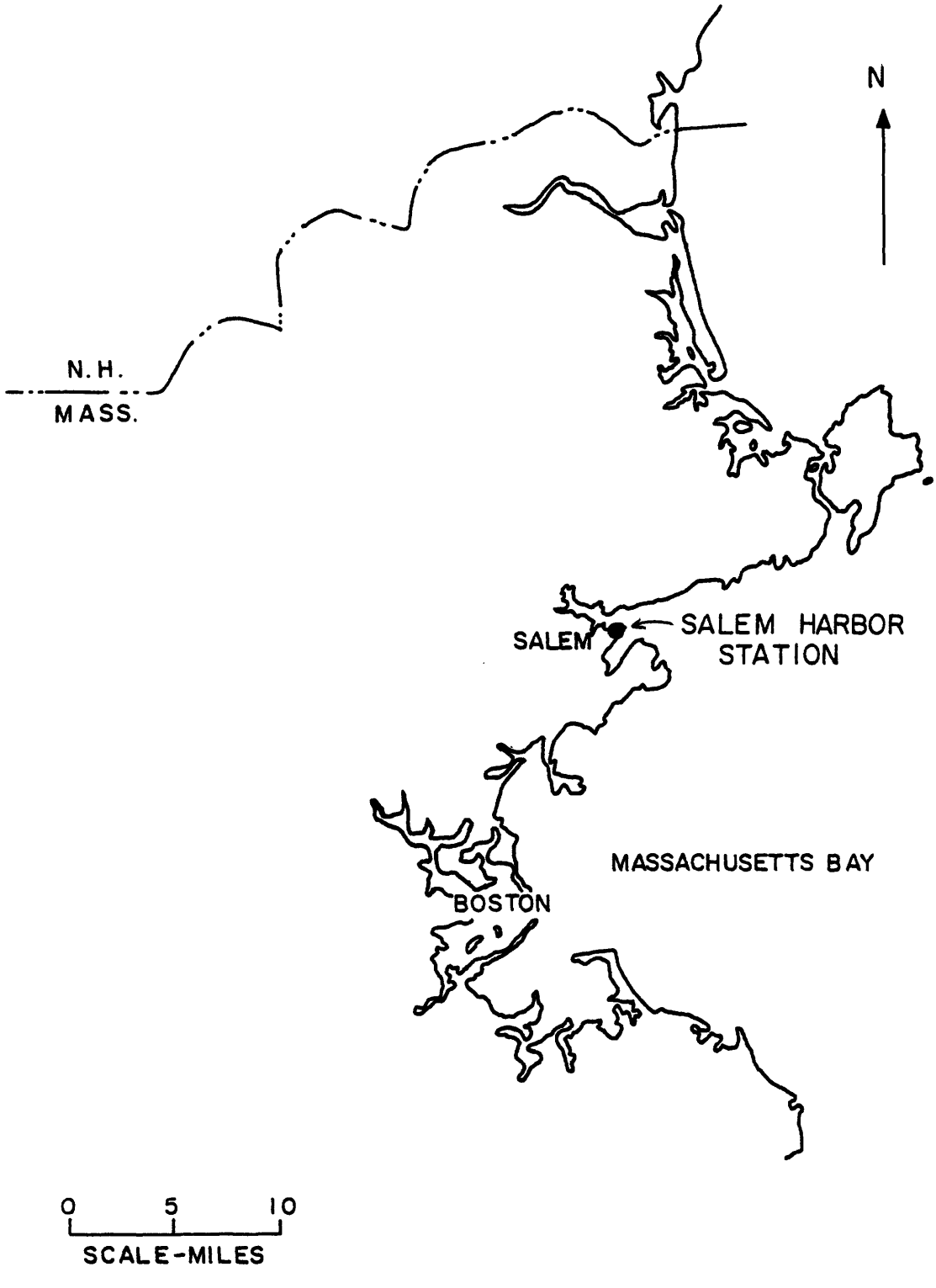

FIGURE I-1 GENERAL VICINITY OF SALEM HARBOR STATION

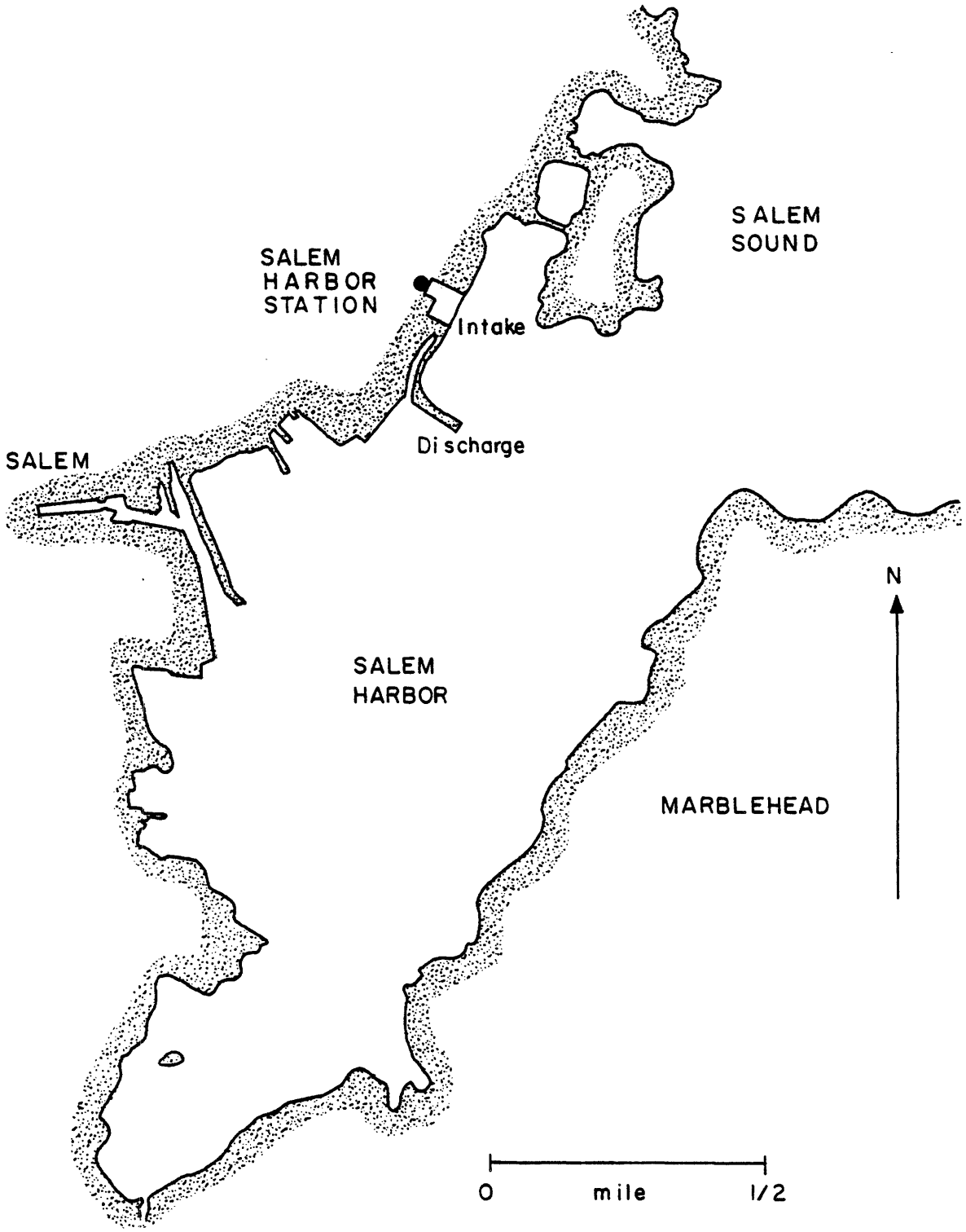

FIGURE 1-2 SALEM HARBOR STATION AND ADJACENT WATER BODIES

normal cooling water. This recirculated heat adds an increment to the total discharge temperature. Crawford (personal communication) suggests that if generation is reduced late at night, the power plant could produce more power the next evening during peak demand, since the intake water would be cooler. Experiments by Kenison and Galli (1975) support this suggestion.

This approach to generation control is economically attractive because make-up power is cheaper late at night than during peak demand periods (1$ - 2/MWH vs. $5 - 10/MWH). The proposed STF system allows economic generation control, by determining the nighttime load reduction necessary to ensure that the discharge stays below T_{max} during the next day's peaking time. The system also computes the net savings from following the recommended load pattern instead of that originally forecast. The relationship between discharge temperature, power production, and power costs is depicted for a hypothetical case in Figure 1-3, showing the potential advantage of STF. Figure 1-4 summarizes the STF system in flow-chart form.

The STF system for power plant discharge control can be broken down into three principal components:

1. An accurate model of intake temperatures as a function of previous discharge temperatures and other environmental factors:

   $T_{in} = f_1(T_{out}$, environmental variables)

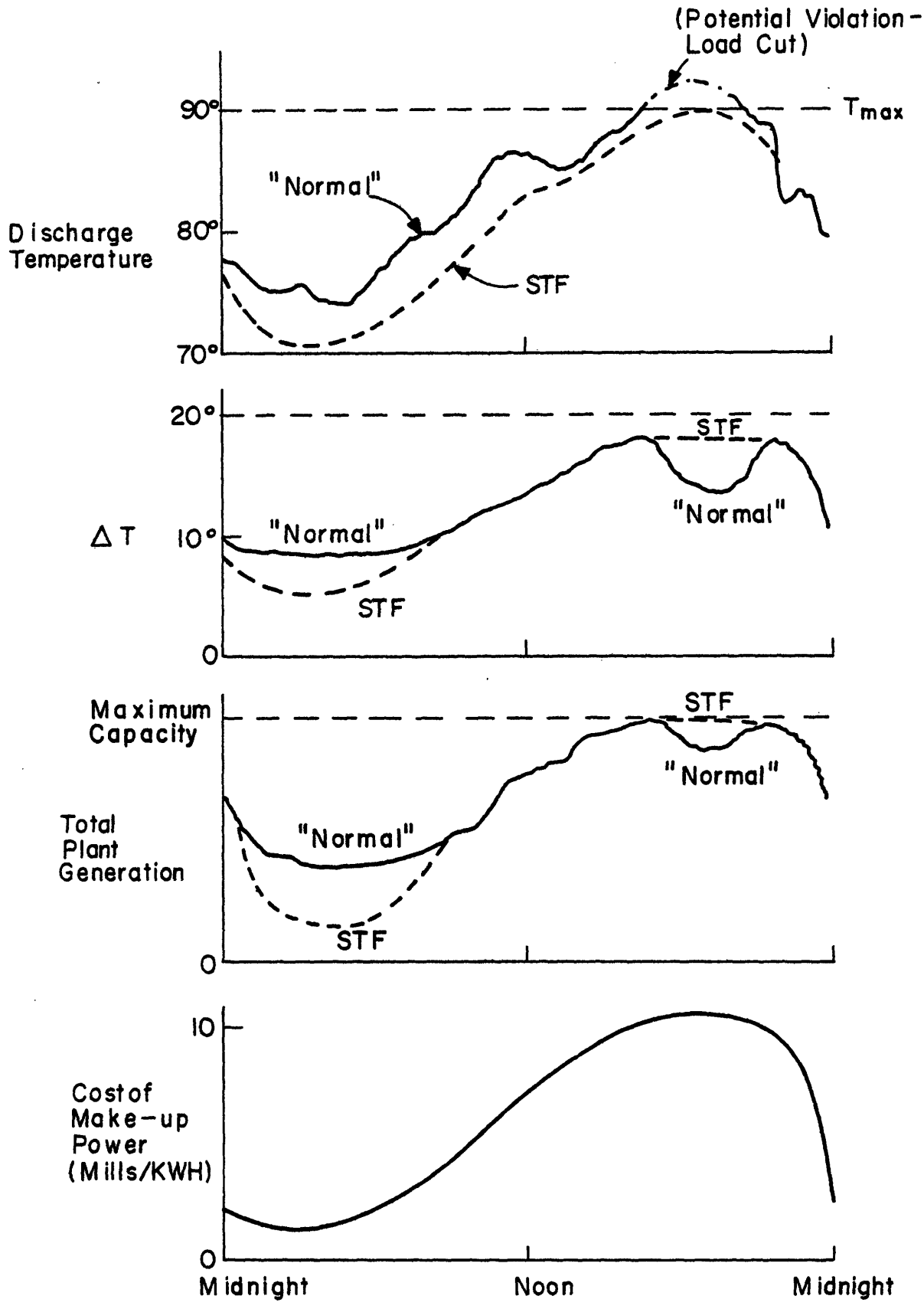

FIGURE 1-3 HYPOTHETICAL EXAMPLE OF STF OPERATION

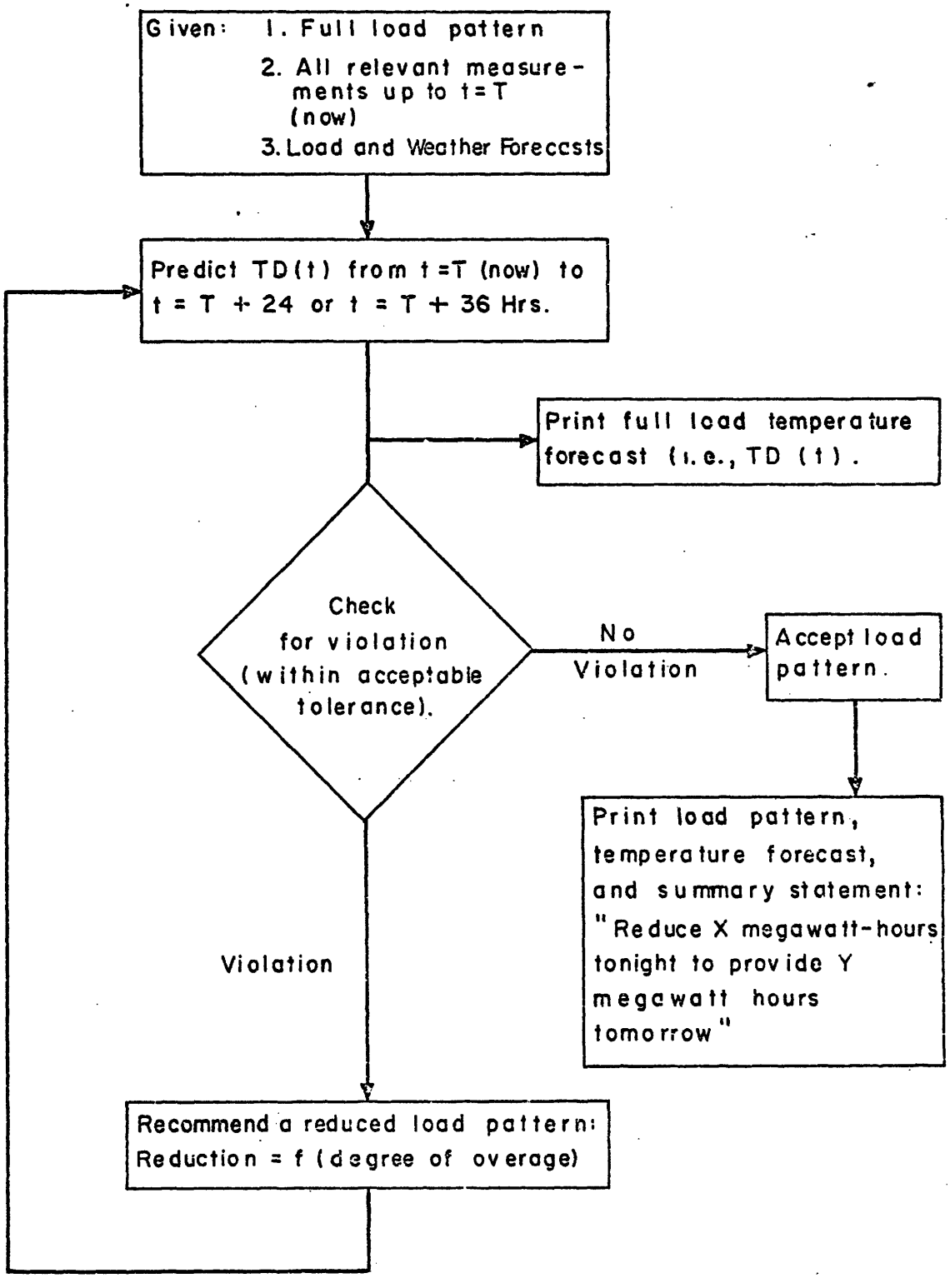

FIGURE 1-4: FLOW CHART OF STF SYSTEM

2. An accurate model of ΔT (from intake to discharge) as a function of plant operating characteristics: $\Delta T = f_2$(plant operations)

3. Control laws for the optimal control of plant operations under existing economic and environmental objectives.

Because $T_{out} = T_{in} + \Delta T$, one can combine the models from 1 and 2. This yields a recursive model of T_{out} as a function of environmental factors (which one cannot control) and plant operations (which one can control):

$$T_{out}(n+1) = f_3[T_{out}(n,n-1,\ldots), \text{Environment } (n,n-1,\ldots), \text{Plant operations } (n,n-1,\ldots)].$$

Control laws use this model to define minimum-cost plant-operation schedules which ensure $T_{out} \leq T_{max}$.

STF forecasts of discharge temperatures must be fairly accurate to achieve economic control of generation. The risk is that a costly night-time load reduction, recommended by the STF system, may not be necessary to meet discharge limitations. Kenison and Galli (1975), estimate that the predicted peak temperature for the next day must be accurate to within $\pm$ 1°F of the actual, 90% of the time, to justify using the STF system. (This is a subjective estimate; probabilistic analysis of expected savings with this system might show a lower accuracy to be acceptable).

To minimize STF operating costs, the system must employ computer programs which are small and inexpensive to run. This also encourages a simple system which is easy for field personnel to understand.

1.2 The Model Development Problem

An STF system requires a model of intake water temperatures at Salem Harbor Station. From the preceding background discussion, the model development problem may be stated as follows:

> Develop a simple and accurate model of intake temperatures at Salem Harbor Station. The model must predict up to 24 hours into the future. It must predict the daily peak intake temperature within $\pm$ 1°F, 90% of the time. It must be developed using existing data from Salem Harbor.

The present study focuses on this model development problem. Development of other STF components is not treated herein.

Considerable data exists on the hydraulic and thermal behavior of Salem Harbor, providing a good basis for model development and verification. Available data includes three years of hourly records of temperatures, weather, tides, and power plant operations, combined with occasional synoptic temperature measurements (outside Salem Harbor). Appendix B summarizes the types and sources of data available.

1.3 An Estimation-Theoretic Approach

Estimation theory is a unified body of theories and algorithms for estimation of variables in uncertain systems (see Schweppe, 1973). Algorithms exist for obtaining optimal (minimum uncertainty) estimates of: states, initial and boundary conditions, inputs, parameters, and model structures.

These estimation techniques share a common approach to analysis of the uncertainties in a system. Information about a system is acknowledged to exist both in a model of the system and in measurements of the system. It is also acknowledged that there are imperfections in both the model and the data. Under these conditions, a best estimate of the system states, parameters, or other attributes is obtained by combining the information from the model and data. The uncertainty in an estimate can be quantified, and thus an optimal (minimum uncertainty) estimate may be obtained.

This report approaches the above model development problem in estimation-theoretic terms, as a problem in model identification, parameter estimation, and state estimation. The approach to this problem follows that proposed by Schweppe (1973):

1. Hypothesize a model structure
2. Estimate parameters
3. Evaluate the resulting model

To do the estimation, selected tools of estimation theory are employed:

Kalman Filtering - for optimal estimation of states and initial conditions

Full-Information Maximum-Likelihood Parameter Estimation - for optimal parameter estimation.

The type of model development problem examined herein is unique among the water quality modeling literature, in specifying an accuracy criterion for a water quality model of a real system. The only similar study, by Kenison and Galli (1975), treats the same Salem Harbor problem considered herein.

The maximum-likelihood parameter estimation scheme employed in the present study is also unique among water quality models. The closest analog is the work of Young et al (1971) and Young and Whitehead (1974). They develop an Instrument Variable-Approximate Maximum Likelihood (IVAML) method for parameter estimation, and apply it to a river BOD/DO system. The IVAML approach is theoretically suboptimal, but the method may yield near-optimum estimates at potentially lower costs than a full-information maximum-likelihood method. Also related to this work are

the investigations reported by Shastry et al (1973). They employ maximum-likelihood and weighted least-squares methods (without filtering) to estimate the parameters in alternative BOD/DO models.

A variety of other parameter estimation techniques are reported for water quality models. Young and Beck (1974) apply the Extended Kalman Filter to estimate parameters in a BOD/DO system. Water Resources Engineers, Inc. (1973) also employ the Extended Kalman Filter, to estimate ground water basin parameters. Lee and Hwang (1971) use a quasi-linearization approach to estimate BOD/DO model parameters. Ulanowicz et al (date unknown) use a multiple regression to estimate parameters of a Lotka-Volterra plankton population model; in addition, they use the F-values from the regression to identify and delete unimportant terms in the model. Koivo and Phillips (1971) employ a stochastic approximation method to estimate parameters of a BOD/DO system, in both simulated and real rivers. Koivo and Philips (1972) obtain least-squares estimates of BOD/DO model parameters, again for both simulated and real rivers.

Though unfamiliar to water quality modeling, experience with maximum-likelihood parameter estimation is common in other applications, such as aeronautics (Rault, 1973), industrial processes (Gustavsson, 1973) and electric power systems (Baeyens and Jacquet, 1973).

The software for optimal filtering and maximum-likelihood parameter estimation in this study is provided by GPSIE - "General Purpose System Identifier and Evaluator" - developed by Peterson and Schweppe (1974). GPSIE is a powerful model development tool offering, among

other options: simulation, optimal filtering, maximum-likelihood parameter estimation (including several non-linear optimization routines), plotting, bad data detection, and calculation of various measures of model performance (such as whiteness-of-residuals, the hessian at the optimal parameter estimate, etc.). GPSIE can be used in either interactive or batch mode, and is applicable to any model in linear, state-space, white-process form. Petersen (1975) applies GPSIE in developing a dynamic model of U.S. energy demand.

1.4 Policy Aspects of an STF System

The ultimate utility of a new environmental control technology is determined by its fit with applicable environmental policy. Thus, in conjunction with developing a new technology, it is wise to explore the policy aspects of the proposed work. Policy issues associated with an STF system are analyzed in Schrader (1976). Environmental impacts and economic benefits of STF are uncertain, but appear to be low. Therefore, use of STF (if this occurs) is not expected to raise policy issues.

1.5 Objectives

To summarize the foregoing discussion, this study has two objectives:

1. Solve the STF model development problem posed above, i.e., develop a simple model of intake temperatures at Salem Harbor Station that predicts the daily peak intake temperature within 1°F, 90% of the time.

2. Apply optimal filtering and maximum likelihood parameter estimation to a water quality model of a real system using field data. Evaluate the advantages and disadvantages of using these techniques in this application.

1.6 Overview of Contents

To introduce the estimation methods used in the model development process, Chapter 2 presents a review of state and parameter estimation. Chapter 3 presents alternate model structures for this problem, and describes the structure ultimately selected. In Chapter 4, estimation methods are applied to the appropriate model structure. Chapter 4 presents the results of the estimation process, and evaluates the performance of the resulting model. Chapter 5 presents a summary, conclusions, and recommendations.

CHAPTER TWO

STATE AND PARAMETER ESTIMATION METHODS

This chapter reviews the state and parameter estimation methods used to develop the model of intake water temperatures. This review explains (qualitatively) the mathematical tools used herein, and establishes a basis for interpreting the usefulness of these tools. The chapter presents only the basic concepts of how the estimation methods work; the reader is referred to Schweppe (1973) for complete derivations.

2.1 Review of Optimal Filtering and Maximum-Likelihood Parameter Estimation

Fundamental to most of estimation theory is the State-Space, White Process Model for uncertain dynamic systems (Schweppe, 1973). For the linear, time-varying case, this form is:

$$\underline{x}(n) = \underline{\underline{F}}(n-1)\underline{x}(n-1) + \underline{\underline{B}}(n-1)\underline{u}(n-1) + \underline{w}(n-1)$$

$$\underline{z}(n) = \underline{\underline{H}}(n)\underline{x}(n) + \underline{v}(n)$$

where: $\underline{x}(n)$ = vector of state variables at time n

$\underline{\underline{F}}(n)$ = state transition matrix

$\underline{u}(n)$ = vector of deterministic, exogenous inputs

$\underline{\underline{B}}(n)$ = matrix of input gains

$\underline{w}(n)$ = vector of model noise

$\underline{z}(n)$ = vector of measurements (or "observations")

$\underline{\underline{H}}(n)$ = measurement matrix

$\underline{v}(n)$ = vector of measurement noise

Model noise, measurement noise, and uncertain initial conditions are modeled as follows:

$$E[\underline{x}(o)] = x_o \qquad E[\underline{w}(n)] = \underline{0} \qquad E[\underline{v}(n)] = \underline{0}$$

$$E[\underline{x}(o)\underline{x}'(o)] = \underline{\underline{\Psi}} \qquad E[\underline{w}(m)\underline{w}'(n)] = \begin{cases} \underline{\underline{Q}}(n), & m=n \\ \underline{\underline{0}}, & m \neq n \end{cases} \qquad E[\underline{v}(m)\underline{v}'(n)] = \begin{cases} R(n), & m=n \\ \underline{\underline{0}}, & m \neq n \end{cases}$$

$$E[\underline{x}(o)\underline{w}'(n)] = \underline{\underline{0}} \qquad E[\underline{x}(o)\underline{v}'(n)] = \underline{\underline{0}} \qquad E[\underline{w}(m)\underline{v}'(n)] = \underline{\underline{0}} \text{ All } m,n$$

Future estimates of the state-vector are predicted using this model. The error covariance $\underline{\underline{\Sigma}}$ is a measure of the uncertainty in the state estimate:

$$\underline{\underline{\Sigma}}(n) = E[(\underline{x}(n) - \hat{\underline{x}}(n))\ (\underline{x}(n) - \hat{\underline{x}}(n))']$$

where: $x(n)$ = true value of state vector

$\hat{x}(n)$ = estimated state vector

$E[\ ]$ = expectation operator.

Schweppe (1973) shows that $\underline{\underline{\Sigma}}$ is given by:

$$\underline{\underline{\Sigma}}(n) = \underline{\underline{F}}(n-1)\ \underline{\underline{\Sigma}}(n-1)\underline{\underline{f}}'(n-1) + \underline{\underline{Q}}(n-1)$$

$$\underline{\underline{\Sigma}}(o) = \underline{\underline{\Psi}} \ .$$

Measurements can also yield an estimation of the state. In applications to real systems, neither the model nor measurements is perfect; thus the resulting state estimate from either will be uncertain. The "filtering" result of estimation theory provides a method for optimally combining the information in the model and the measurements. The

filtered state estimate that is produced has less uncertainty than an estimate based on either model or measurements alone; optimal filtering (also called Kalman Filtering) yields the minimum-variance state estimate (Schweppe, 1973).

A heuristic explanation of the filtering process is as follows:

1. Begin at time n with a filtered state estimate incorporating measurements through time n: $\hat{\underline{x}}(n|n)$. Predict the state at time n+1:

$$\hat{\underline{x}}(n+1|n) = \underline{\underline{F}}(n)\,\hat{\underline{x}}(n|n) + \underline{\underline{B}}(n)\underline{u}(n)$$

This is the best estimate of $\underline{x}(n+1)$ based on the model alone. The uncertainty in this estimate is:

$$\underline{\underline{\Sigma}}(n+1|n) = \underline{\underline{F}}(n)\underline{\underline{\Sigma}}(n|n)\underline{\underline{F}}'(n) + \underline{\underline{Q}}(n)$$

2. Take a measurement at time n+1: $\underline{z}(n+1)$. A state estimate based solely on this measurement is (Schweppe, 1973):

$$\hat{\underline{x}}(n+1) = [\underline{\underline{H}}'(n+1)\underline{\underline{R}}^{-1}(n+1)\underline{\underline{H}}(n+1)]^{-1}\,\underline{\underline{H}}'(n+1)\underline{\underline{R}}^{-1}(n+1)\underline{z}(n+1)$$

The uncertainty in this estimate is:

$$\underline{\underline{\Sigma}}(n+1) = [\underline{\underline{H}}'(n+1)\underline{\underline{R}}^{-1}(n+1)\underline{\underline{H}}(n+1)]^{-1}$$

3. Estimate $\hat{\underline{x}}(n+1|n+1)$. The filtered estimate (or "updated" estimate) is a weighted average of the state estimate based on the model and the estimate based on the measurement. The weighting scheme is determined by the relative uncertainty of the two estimates (Schweppe, 1973):

$$\hat{\underline{x}}(n+1|n+1) = \underline{\underline{\Sigma}}(n+1|n+1)[\underline{\underline{H}}'(n+1)\underline{\underline{R}}^{-1}(n+1)\underline{z}(n+1) + \underline{\underline{\Sigma}}^{-1}(n+1|n)\underline{x}(n+1|n)]$$

The uncertainty in the filtered estimate is:

$$\underline{\underline{\Sigma}}\ (n+1|n+1) = [\underline{\underline{H}}'(n+1)\underline{\underline{R}}^{-1}(n+1)\underline{\underline{H}}(n+1)\ \underline{\underline{\Sigma}}^{-1}(n+1|n)]^{-1}$$

Note that this uncertainty is less than either $\underline{\underline{\Sigma}}(n+1|n)$, the uncertainty in the model estimate, or $\underline{\underline{\Sigma}}(n+1)$, the uncertainty in the measurement estimate.

The model parameters are the variables in the model which are independent of the states and the inputs. In the State-Space, White Process Model, the parameters include the initial conditions $\underline{x}_o$; the elements of the matrices $\underline{\underline{F}}(n)$, $\underline{\underline{H}}(n)$, and $\underline{\underline{B}}(n)$; and the elements of the covariance matrices $\underline{\underline{Q}}(n)$ and $\underline{\underline{R}}(n)$. If some of these parameters are unknown or poorly known, they may be estimated from measurements on the system. Maximum-likelihood parameter estimation is a tool for obtaining optimal parameter estimates under conditions of uncertainty in the model and measurements.

The previous model can be re-written to indicate that it incorporates uncertain parameters, which are to be estimated:

$$\underline{x}(n) = \underline{\underline{F}}(\underline{\alpha},n+1)\ \underline{x}(n-1) + \underline{\underline{B}}(\underline{\alpha},n-1)\underline{u}(n-1) + \underline{w}(n-1)$$

$$\underline{z}(n) = \underline{\underline{H}}(\underline{\alpha},n)\underline{x}(n) + \underline{v}(n)$$

where $\underline{\alpha}$ = vector of unknown parameters.

Maximum-likelihood parameter estimation is essentially an iterative searching procedure over alternate parameter estimates $\underline{\alpha}_j$. Define the vector of all observations through time n:

$$\underline{z}_n = \begin{bmatrix} \underline{z}\ (1) \\ \cdot \\ \cdot \\ \cdot \\ \underline{z}(n) \end{bmatrix}$$

Then the overall maximum-likelihood parameter estimation procedure is as follows (see Schweppe, 1973):

1. Propose a parameter estimate $\underline{\alpha}_j$
2. Run the model through time n, using $\underline{\alpha} = \underline{\alpha}_j$
3. Compute the likelihood $\ell(\underline{\alpha}_j | \underline{z}_n)$ of model j. (Note that $\ell(\underline{\alpha}_j | \underline{z}_n) = P_j[\underline{z}_n]$, the probability that the observations $\underline{z}_n$ would be generated by model j.)
4. Propose a new $\underline{\alpha}_k$ and repeat, until the $\underline{\alpha}_i$ with the maximum likelihood is obtained.

The key step in this process is the computation of the likelihood. A recursive method is described below which employs a filtering algorithm to generate optimal state estimates for the likelihood computation. By definition of conditional probability:

$$P_j[z_n] = P_j[\underline{z}(n) | \underline{z}_{n-1}] \cdot P[\underline{z}_{n-1}]$$

For convenience, the log-likelihood is considered, instead of the likelihood itself:

$$\begin{aligned} \text{Log-likelihood} = \xi_j(n) &= \ell n\ P_j\ [\underline{z}_n] \\ &= \ell n\ P_j\ [\underline{z}(n) | \underline{z}_{n-1}] + \ell n\ P_j[\underline{z}_{n-1}] \\ &= \ell n\ P_j\ [\underline{z}(n) | \underline{z}_{n-1}] + \xi_j(n-1) \end{aligned}$$

where $\xi_j(o) = 0$.

If one assumes that the noise processes $\underline{x}_o$, $\underline{w}(n)$ and $\underline{v}(n)$ are all Gaussian, then the conditional probability distribution $P_j[\underline{z}(n) | \underline{z}_{n-1}]$

is Gaussian, and can be computed for any value of $\underline{z}(n)$ (Schweppe, 1973). Taking the log of this distribution, and multiplying across by 2, one obtains:

$$2 \ln P_j[\underline{z}(n)|\underline{z}_{n-1}] =$$
$$-k \ln 2\pi - \ln[\det \underline{\underline{\Sigma}}_z (n|n-1)] - \underline{\delta}_z' (n) \underline{\underline{\Sigma}}_z^{-1} (n|n-1) \underline{\delta}_z (n)$$

where:

k = dimension of $\underline{z}(n)$

$\underline{\delta}_z(n)$ = measurement residual

$= \underline{z}(n) - \hat{\underline{z}}(n|n-1) = \underline{z}(n) - \underline{\underline{H}}(n) \hat{\underline{x}} (n|n-1)$

$\underline{\underline{\Sigma}}_z (n|n-1)$ = covariance of measurement residual

$= \underline{\underline{H}} (n) \underline{\underline{\Sigma}} (n|n-1) \underline{\underline{H}}' (n) + \underline{\underline{R}} (n)$

The residual $\underline{\delta}_z(n)$ is computed at each time step from $\hat{\underline{z}}(n|n-1)$, which is in turn a one-step prediction from $x(n-1\ n-1)$. Likewise, $\underline{\underline{\Sigma}}_z (n|n-1)$ is computed directly from the filter results for time n-1, $\underline{\underline{\Sigma}} (n-1|n-1)$.

In summary, the recursive algorithm for computing model likelihood in one pass through the data is:

1. Given $\xi_j(n-1)$, $\hat{\underline{x}}(n-1|n-1)$ and $\underline{\underline{\Sigma}} (n-1|n-1)$, predict $\hat{\underline{z}}(n|n-1)$ and $\underline{\underline{\Sigma}}_z (n|n-1)$.

2. Use $\underline{z}(n)$ with $\hat{z}$ $(n|n-1)$ and $\underline{\underline{\Sigma}}_z$ $(n|n-1)$ to compute $\ln P_j[z(n)|z_{n-1}]$, and add to $\xi_j(n-1)$ to get $\xi_j(n)$.

3. Use $\underline{z}(n)$ with optimal filter to update model: $\hat{\underline{x}}(n|n)$ and $\underline{\underline{\Sigma}}$ $(n|n)$.

The likelihood calculated in this way employs all information available on the modeled system, and is called the "full-information" likelihood in this thesis. The estimation method is called "Full-Information Maximum Likelihood" (FIML) estimation.

2.2 Alternate Measures of Model Performance

The model development problem posed in Chapter One specifies that the error in daily (24-hour) peak temperature predictions shall be less than 1°F, in 90% of the predictions. The implied measure of performance is computed as follows:

1. From initial conditions, make an unfiltered forecast of intake temperatures over the next 24 hours.

2. Compute the error between the predicted and observed peak temperatures for this period.

3. Repeat steps 1 and 2 for m consecutive 24-hour periods.

This measure of performance is T, defined as:

> T = percentage of 24-hour periods for which the error in peak intake temperature prediction is less than or equal to 1°F.

The model development problem specifies the accuracy criterion:

$$T \geq 90\%.$$

The full-information likelihood is a different measure of model performance, not strictly equivalent to T. One important difference is that the full-information likelihood involves updating of the model at every time step (via optimal filtering), whereas T involves an un-updated, 24-hour prediction. A second difference is that the full-information likelihood incorporates prediction-measurement discrepancies at every time-step in a 24-hour period, whereas T only accounts for the discrepancy in peak temperatures in any 24-hour period. In qualitative terms, T is a measure of the fit of the model to daily peak temperatures,

when the model is updated (re-initialized) once every 24 hours. By comparison, the full-information likelihood is a measure of the model's fit to the complete stream of hourly temperatures, when the model is updated every hour.

A variety of other measures of model performance also suggest themselves. Several of the measures are used to evaluate model performance in Chapter Four:

1. Sum of squares of normalized measurement residuals, S:

$$S = \sum_{i=1}^{m} \sum_{n=1}^{24} [\underline{\delta}_z'(n) \, \underline{\underline{\Sigma}}^{-1} (n|n-1) \, \underline{\delta}_z(n)]$$

where m = number of days.

Schweppe (1973) shows that for a perfect model, S is a chi-square distributed variable with d degrees of freedom:

$$S \cong \chi^2(d, 2d)$$

where $d = (24 \cdot m \cdot k) - h$

h = dimension of $\underline{\alpha}$

The variance of S is $\sigma_S^2 = 2d$.

These results are helpful for distinguishing local from global maxima on the likelihood surface. If $S_j \neq E[S] \pm 2\sigma_S$ there is reason to doubt the validity of the model with parameters $\underline{\alpha}_j$. It may be that one's initial estimates for $\underline{\underline{Q}}$ and $\underline{\underline{R}}$ are too large. This will inflate $\underline{\underline{\Sigma}}_z$, thereby reducing S and artificially improving ξ. Thus, a false maximum-likelihood point may be located. Improved estimates of $\underline{\underline{Q}}$ and $\underline{\underline{R}}$ are ones sufficiently low to make $S \cong F[S]$, if possible. A second maximum-likelihood estimation, using improved $\underline{\underline{Q}}$ and $\underline{\underline{R}}$, will yield better

estimates of $\underline{\alpha}$. (This measure of performance applies only to fully updated models).

2. Mean-square Error of Predicted Hourly Temperatures, M:

$$M = \frac{1}{m} \sum_{i=1}^{m} \{\frac{1}{24} \sum_{n=1}^{24} [\hat{z}(n|1) - z(n)]^2\}$$, where z = intake temperature

For each day i, an unfiltered 24-hour forecast is made (just as would be done using the STF system). The mean-square error of the hourly predictions is computed, and averaged over m days. M is an absolute measure of the error in a prediction. However, it can give an erroneous estimate of model accuracy if used alone, because it fails to account for potential measurement errors and random variations in inputs.

3. Mean-square Error of Predicted Daily Peak Temperatures, D:

$$D = \frac{1}{m} \sum_{i=1}^{m} [\hat{z}_i^* - z_i^*]^2$$

where $\hat{z}_i^*$ and z_i^* are the predicted and measured peak intake temperatures, respectively, for day i. Unfiltered 24-hour forecasts are used to generate $\hat{z}_i^*$. D is related to T. If one assumes that the error, ε, in peak temperature predictions is normally distributed, $\varepsilon \sim N(o,\sigma_\varepsilon^2)$, then D is an estimate of σ_ε^2. Under this assumption, to achieve $T \geq 90\%$, one must achieve $D \leq 0.78$.

4. Normalized Whiteness of Residuals, P(a):

Peterson (1975) defines the whiteness test matrix:

$$P(a)_{ik} = (R(a)_{ik} - E[R(a)_{ik}])/\sigma_{R(a)_{ik}}$$

where $P(a)_{ik}$ = number of standard deviations by which the ikth element of the whiteness matrix differs from its expected value.

$$\underline{\underline{R}}(a) = \frac{i}{N-a} \sum_{n=1}^{N-a} [\tilde{\underline{\delta}}_z'(n)\tilde{\underline{\delta}}_z (n+a)]$$

= whiteness matrix for lag a

$$\tilde{\underline{\delta}}_z(n) = \underline{\underline{\Sigma}}_z^{-1/2} (n|n-1)\underline{\delta}_z(n)$$

$$\sigma_{R(a)_{ik}} = \begin{cases} \sqrt{2/N}, & \text{for } R(o)_{ii} \\ \sqrt{1/N}, & \text{for } R(o)_{ik},\ i \neq k \\ \sqrt{1/N - a/N^2}, & \text{for } R(a),\ a \neq o \end{cases}$$

$$E[\underline{\underline{R}}(a)] = \begin{cases} \underline{\underline{I}}, & a = 0 \\ \underline{\underline{0}}, & a \neq 0 \end{cases} \quad \text{for perfect model}$$

Peterson (1975) indicates that this is an extremely sensitive measure of model performance. He suggests as a rule of thumb that the elements of $\underline{\underline{P}}(0)$, $\underline{\underline{P}}(1)$, $\underline{\underline{P}}(2)$ and $\underline{\underline{P}}(3)$ should be less than four or five, to indicate an acceptable model. This measure of performance applies only to fully updated models.

5. Covariance of 24-hour Predicted Temperature, $\sigma_z^2 (n + 24|n)$:

$\sigma_z^2 (n + 24|n)$ = ith diagonal element of $\underline{\underline{\Sigma}}_z (n + 24|n)$ for which z_i = intake temperature

Note that $\sigma_z^2(n + 24|n)$ is not constant, but a function of n.

Although the model development problem is posed in terms of T, parameter estimation is done using the full-information maximum-likelihood criterion. This choice is made for several reasons. First, the full-information likelihood incorporates into the parameter estimation all available information about the system. The off-peak behavior of the system contains useful information for model development, which T ignores. Second, because it is derived from probabilistic assumptions about the modeled system, the maximum-likelihood approach allows one to infer how well the resulting parameter estimate will perform on data not included in the estimation. If the probabilistic assumptions are true, then the full-information maximum-likelihood parameter estimate is the optimal estimate (Schweppe, 1973). Under these conditions, maximizing the full-information likelihood is sufficient (but not necessary) to maximize T.

In addition to being theoretically optimal, the full-information maximum-likelihood approach offers other advantages. By modelling the full, hourly behavior of the system, one automatically solves the problem of predicting the time of peak intake temperature. The time of the peak is needed (fairly accurately), so that the STF system may determine temperature-control measures with reasonable confidence. A parameter estimation based on T requires additional manipulation to fit time-of-peak records, which may be impossible without reducing T.

Cost is also a factor in the present case, wherein a full, hour-by-hour filtering algorithm is required to initialize the model each day (see Appendix C). The full-information likelihood (using the

filtering results also used to initialized the model) incorporates 24 data points for each day, compared to 1 data point per day (i.e., the peak temperature) for T. Thus, an estimation using T must span 24 times as many days as one using the full-information likelihood, to have the same "size" data base. If the same model (with full filtering for initial conditions) is used in both estimations, the estimation using T requires roughly 24 times more computation than one using the full-information likelihood. (The opposite would be true if full filtering for initial conditions were not required).

One further advantage of this approach is that computational delay and inconvenience are minimized by GPSIE, which offers fully-implemented routines for full-information maximum-likelihood parameter estimation.

2.3 Optimization Procedure

For a given set of data, $\underline{z}_n$, the log-likelihood is a non-linear function of α_j:

$$\xi(n) = f(\underline{\alpha}_j | \underline{z}_n)$$

Maximum-likelihood parameter estimation requires an iterative search for the values of $\underline{\alpha}$ which maximize $\xi(n)$. This is essentially a non-linear optimization problem, for which a variety of solutions exist (see Aoki, 1971). The present study uses a method originally proposed by Powell (1964) and refined by Zangwill (1967), for minimizing a function without calculating derivatives.

The basic approach of the Powell search is to iteratively revise a set of orthogonal search directions, until a set of directions is found along which no further increase in the function can be achieved. See Zangwill (1967) for the detailed search algorithms. Zangwill proves that this method converges to the minimum of any strictly convex function. By symmetry, the method is equally valid for finding the maximum of a strictly concave function.

It is impossible to define *a priori* which optimization procedure is best for the maximum-likelihood identification problem at hand. The shape of the log-likelihood function, $\xi(n) = f(\underline{\alpha}_j | \underline{z}_n)$, is not generally known *a priori*. The function may be multi-modal, in which case no optimization procedure can assure the user of finding the global maximum. Thus, selection of an optimization procedure is based on the user's intuition about the problem and about the solution procedures available. The Powell search is chosen for the present study mainly because of

Peterson's (1975) success using the method on a 20-variable FIML parameter estimation. Also, the Powell search is potentially less expensive than gradient searches for cases initialized relatively near the optimum point. The Powell search is also chosen because it is conveniently available on GPSIE. (Also available, but not used in this study, are the Newton Search (see Aoki, 1971) and Davidon-Fletcher-Powell Search (Fletcher and Powell, 1963)).

This concludes a review of the tools used for state and parameter estimation in this study. The following chapter develops the basic model, to which these tools are applied.

CHAPTER THREE

MODEL STRUCTURE

3.1 Alternate Model Structures

A taxonomy of possible models for Salem Harbor is presented in Figure 3-1. Two basic model structures are considered, representing fundamentally different approaches to model development. In the statistical approach, states and/or measurements of interest are viewed as random processes, outputs of a stochastic input-output system. A model, in this paradigm, is perceived as a relation between the inputs and outputs. Model development consists of iteratively revising these relations, in an effort to explain as much as possible of the variance of the output process(es). Such models may also be termed empirical.

In the physically-derived approach, states, inputs, and measurements are perceived to be related to each other by deterministic laws reflecting causality. Model development, in this paradigm, consists of finding the true value of weakly known parameters, and the true representation of causal mechanisms.

There are advantages to each approach. The advantage of statistical models is their relative algebraic simplicity, making the dynamic relationships between the variables clearer than in physically-derived models. The structural modifications necessary to achieve a desired output are thus easier to perceive. Although more complex, physically-derived models offer the advantage of incorporating all of one's intuition and experience about the system being modeled.

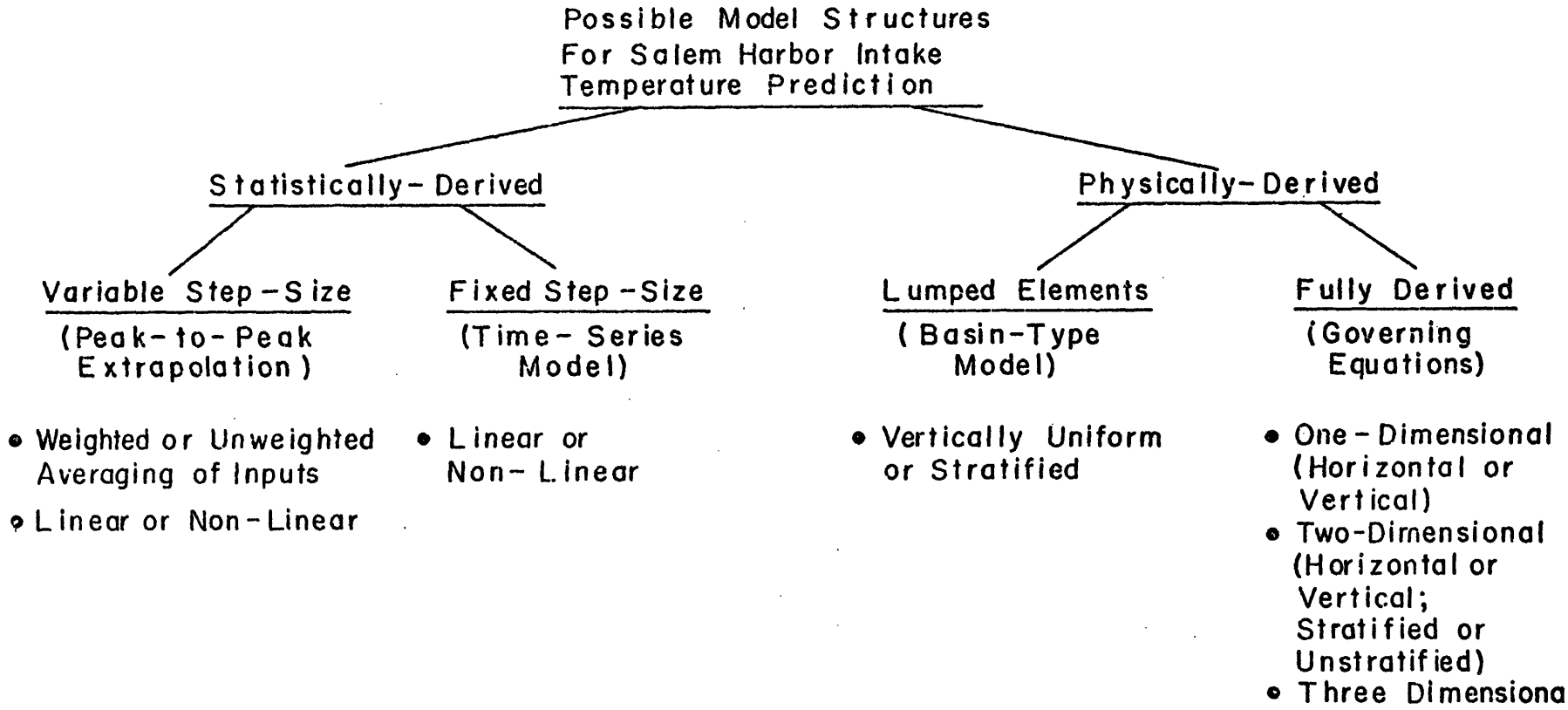

FIGURE 3-1 A TAXONOMY OF MODEL STRUCTURES

This thoroughness facilitates modeling of systems for which little or no operating data is available.

Statistical models of water quality are uncommon. One likely reason is that an adequate data base at any one site is rare. Also, statistical models do not build from comprehensive, general laws, in contrast to most water quality models. This unrealistic approach may leave some modelers uncomfortable. Nevertheless, as existing environmental monitoring programs accumulate fairly long records for particular sites, empirically derived models should be considered for some applications.

Two types of statistical models and two types of physically-derived models are considered for the Salem Harbor intake temperature problem (Figure 3-1):

1. "Peak-to-peak extrapolation" models use today's peak intake temperature, plus other weather, tide, and plant generation data, to predict tomorrow's peak intake temperature and the hour in which it will occur. No intervening temperatures are predicted.

2. Time series models predict temperatures at regular time intervals. This is the most general form of statistical model.

3. "Basin-type" models divide the water body into a suitable number of cells (or "lumped elements"), and use physical principles of mass and energy transfer between cells to predict cell temperatures at fixed time intervals. As defined here, basin-type models do not explicitly observe the conservation of momentum; water flow between cells is governed by flows at the boundaries and by assumptions on cell depth.

4. Fully physically-derived models are derived from the governing equations of fluid flow. These models are essentially numerical solutions of the governing equations, suitably discretized in space and time, and with suitable assumptions. The details of each model type are assembled in Table 3-1.

A physically derived, basin-type model structure is selected for the present study. Statistical structures are rejected because their potential accuracy appears too low (Table 3-1). The basin-type model appears to offer a higher chance for success, by incorporating a more refined representation of the suspected dominant physical processes (tide, wind, surface heat exchange, plant operation, and stratification). A fully physically-derived model of harbor temperatures is rejected because: 1) it appears to be too complex and expensive to meet the original objective of a simple model; 2) there is doubt whether such complexity will in fact enhance accuracy, or whether this complexity will introduce more uncertainty than it eliminates.

The basin-type model offers an intermediate level of refinement: simpler than a fully physically-derived model, yet incorporating more physical intuition than statistical models. The choice assumes that a simple, physically-derived treatment of the dominant physical processes, "tuned" by optimal estimation of parameters, will yield sufficient accuracy with sufficient simplicity. The specifics of the resulting model structure are described in the following section.

Table 3-1: Alternate Model Structures

Model Type - General Structure	Major Variations	Advantages	Results of Previous Models
Peak-to-Peak Extrapolation $T_{in,peak}$(day i) = f[weighted avg's.of $T_{in,peak}$(day i-1), plant operations, sun, wind, tide]	1) Various weightings, i.e. -peak value over day -value at given hour -uniform/non-uniform weighting over time 2) f(weighted avg's.) may be linear or non-linear	1) If f () is linear, optimal estimation of coefficients is easily done via multiple linear regression. Though sub-optimal and less convenient, non-linear regression may be used if f () or the weighting functions are non-linear. 2) Conceptually simple - can provide basis for subjective estimates by a human predictor (i.e., estimates based on a person's "feel" for what would happen.	1) A subjective/intuitive model predicted next-day peak intake temperature, over June-July, 1974, with following accuracy: ± 1°F, 43% of predictions ± 2°F, 63% of predictions predictions were function of data cited at left. Recorded weather and tides from next-day were used, i.e., perfect forecasts of these variables. See Kenison and Galli (1975). 2) Best univariate non-linear regression, trying various independent variables, predicted next-day peak intake temperature over June-July, 1974: ± 1°F, 11% of predictions See Kenison and Galli (1975). 3) Best multiple linear regression, considering various combinations of independent variables, predicted next-day peak <u>discharge</u> temperature over June-July, 1974: ± 1°F, 34% of predictions See Kenison and Galli (1975).
Fixed-step Time Series Models T_{in} = f[T_{out} (n-1 , n-2,...), sun(n-1, ...), ..., T_{in}(n-1,...)]	1) Various lags and moving-average combinations 2) f () may be linear or non-linear	1) Several packaged computer systems available for developing time-series models: TSP (Harvard Inst. for Econ. Res. 1974), ARIMA methods (Box and Jenkins, 1970) 2) Considerable precedent to build on: Box and Jenkins (1970); Econometric and Hydrologic forecasting work. 3) Amenable to estimation-theoretic techniques (eg. Peterson (1975))	No existing models of this type.
"Basin" Models Derived from conservation of mass and of energy. Equations neglect velocity field (i.e., neglect conservation of momentum). Far-field only.	1) Vertically uniform vs. stratified 2) "Total" temperature vs. "ambient" and "plant-induced"	1) Conceptually simple 2) Computationally simple 3) Do not require detailed information on boundary and initial conditions	**Results of Previous Models** No past experience. Developed in the present study - results presented in Chapter 4.
Fully-Derived Physical Models Derived from conservation of mass, momentum, and energy. Far-field, near-field, or combined.	1) Dimensionality: One (vertical or horizontal), Two (horizontal or vertical), or Three 2) "Total" temperature vs. "ambient" and "plant-induced"	1) Incorporate physical intuition and past experience most thoroughly 2) Equations are "generally applicable" (provided sufficient supporting data and computational capacity is available).	Tsai (personal communication) did a 2-dimensional vertically-averaged finite-difference model of currents and temperatures in Beverly and Salem Harbors. Temperatures are "plant-induced increment over ambient". Point-temperature prediction errors range from 0 to 2°F, over one tidal cycle (no estimate of intake-temperature accuracy). See Appendix B.

3.2 A Simple Two-Basin, Two-Layer Model for Temperature in Salem Harbor

Based on physical principles and past engineering experience with hydrothermal systems, harbor temperatures (on an hourly time scale) appear to be dominated by the following factors: stratification, tides, surface heat exchange, wind, and power plant operations. This is suggested by the subjective-intuitive model of Kenison and Galli (1975), and by inspection of temperature data.

To incorporate these dominant factors in a model, a simple schematization of Salem Harbor (see Figure 3-2) is used. The idealized harbor consists of two basins, each having a surface and a bottom layer. The boundary between the two basins is determined by the breakwater jutting out from the power plant. The harbor is thus broken into four cells, each assumed well-mixed. Across the open boundary from Basin #2 is Salem Sound, also represented by a surface and bottom layer. To simulate harbor temperatures, the model tracks mass and energy tranfers between the cells, the atmosphere, and the sound; conservation of mass and energy are observed. In each time-step, water (and hence, energy) is advected between cells and the sound, according to tidal and power plant flows. Energy is also transferred across the air-water interface. At the end of each time-step, the temperature of each cell is computed; plant intake temperature is then computed from the cell temperatures.

The model thus consists of two finite-difference equations for each cell: an equation for conservation of mass, and an equation

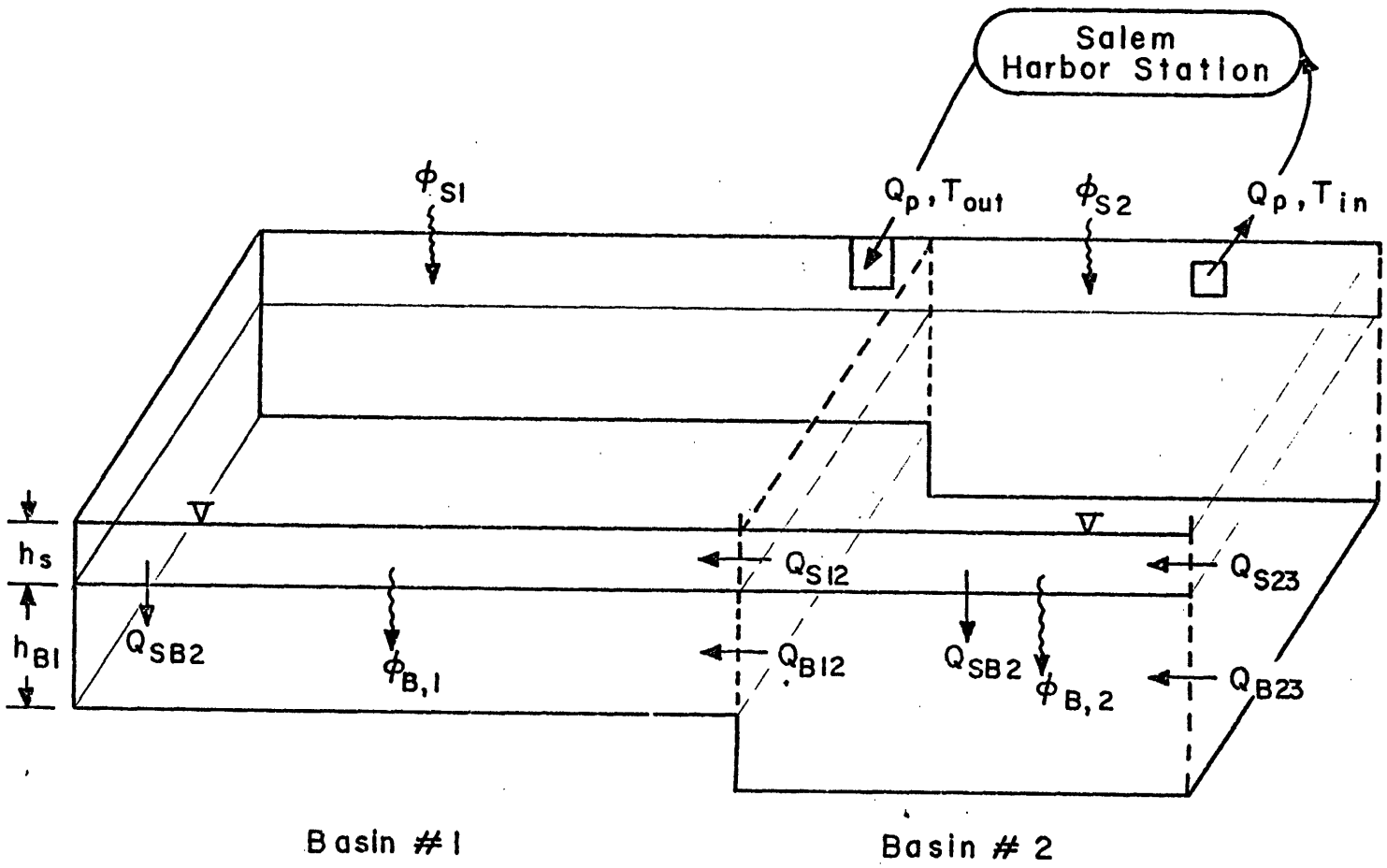

(Note: All Fluxes Positive as Drawn)

FIGURE 3-2 SCHEMATIZATION OF SALEM HARBOR FOR TWO-BASIN, TWO LAYER MODEL

for conservation of energy (the latter yielding cell temperature). The following paragraphs develop these equations, highlighting important assumptions and explaining the unknown parameters to be estimated in Chapter Four. For reference, the resulting equations for each cell are listed at the end of this section in Tables 3-2 and 3-3. A summary list of symbols is also provided at the beginning of the report. Sources of data used for model development are summarized in Appendix B.

3.2.1 Conservation of Mass

Basin #1, Surface Layer:

$$\frac{d}{dt}(V_{S1}) = Q_{S12} - Q_{SB1} + (1 - \gamma)Q_P \qquad (1)$$

where

V_{S1} = Volume of Basin #1, surface layer

Q_{S12} = Flow rate from Basin #2, surface layer into Basin #1, surface layer

Q_{SB1} = Flow rate in Basin #1, from surface to bottom

Q_P = Flow rate through Salem Harbor Station

γ = Plume re-circulation factor (described below)

The heated plant effluent is discharged via a surface discharge canal; hence, the model assumes that all plant discharge enters the surface layers. To allow for plume re-circulation, a fraction γ of the discharge is assumed to enter the surface layer of Basin #2 directly. This re-circulation factor is related to the tide as follows:

$$\gamma = \gamma_2 \qquad \dot{h} > 0$$

$$\gamma = \gamma_2 + \frac{(\gamma_1 - \gamma_2)(-\dot{h})}{5} \qquad \dot{h} \leq 0$$

Thus, for $\gamma_1 > \gamma_2$, re-circulation will reach a maximum at peak ebb tide. γ_2 is a parameter defining the proportion of discharge "normally" entering Basin #2 (during flood tide); γ_1 is a parameter determining the maximum amount of re-circulation at peak ebb.

Q_P is known a priori from planned power plant operating schedules. The area of each basin (A_1 or A_2) is constant, since the harbor is idealized as a rectangular prism. The thickness of the surface layer (h_s) is assumed constant and equal in both basins. (This approximation appears roughly valid for the summer months, based on observed temperature profiles. It is worthy of refinement, however, in later work.)

With these assumptions, the left-hand side above is zero, and

$$Q_{SB1} = Q_{S12} + (1 - \gamma)Q_P \tag{2}$$

Basin #1, Bottom Layer:

$$\frac{d}{dt}(V_{B1}) = Q_{B12} + Q_{SB1} \tag{3}$$

where

V_{B1} = Volume of Basin #1, bottom layer

Q_{B12} = Flow rate from Basin #2, bottom layer into Basin #1, bottom layer.

Recalling that basin area is constant, Eq. (3) becomes:

$$A_1 \frac{d}{dt}(h_{B1}) = Q_{B12} + Q_{SB1} \tag{4}$$

where h_{B1} = depth of bottom layer, Basin #1.

From published tide tables (of the U.S. National Oceanographic and Atmospheric Administration), the tidal height h (relative to mean low water) may be obtained for a given time. Interpolation between high and low tides is done by fitting one-half of a sine wave between each two such points. With a time-step size of 15 minutes or less, this estimated tidal height may be considered uniform throughtout the harbor. The depth of each basin at mean low water is thus:

$$h_{1,min} = h_s + h_{B1,min}$$

$$h_{2,min} = h_s + h_{B2,min}$$

Where $h_{B1,min}$ and $h_{B2,min}$ are the minimum bottom layer depths.

The rate-of-change of tidal height, $\dot{h}$, may be considered uniform throughout the harbor. Thus,

$$\dot{h} = \dot{h}_1 = \dot{h}_S + \dot{h}_{B1} = \dot{h}_{B1} \tag{5}$$

since surface layer thickness is constant. Substituting back into Eq. (4):

$$Q_{B12} + Q_{SB1} = A_1\dot{h} \tag{6}$$

The total tidal flow entering Basin #1 is

$$Q_{12} = Q_{S12} + Q_{B12} = A_1\dot{h} - (1 - \gamma)Q_P \tag{7}$$

A proportion α_1 of this flow enters via the surface layer; thus

$$Q_{S12} = \alpha_1 Q_{12} \text{ , and } Q_{B12} = (1 - \alpha_1)Q_{12} \tag{8}$$

The apportionment of flow is assumed to be related to the relative layer thicknesses:

$$\alpha_1 = b_1\left[\frac{h_S}{h_S + h_{B1}}\right], \text{ and } (1 - \alpha_1) = b_1\left[\frac{h_{B1}}{h_S + h_{B1}}\right] \tag{9}$$

The parameter b_1 is related to the horizontal velocity profile at the boundary of basins 1 and 2:

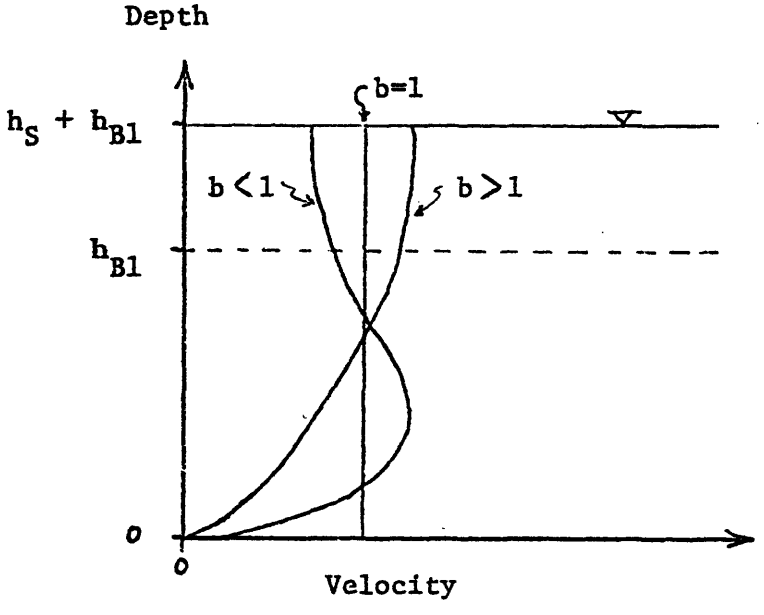

Given b_1, and thus α_1, the inter-cell flows for Basin #1 are:

$$Q_{S12} = \alpha_1[A_1 \dot{h} - (1 - \gamma)Q_P]$$

$$Q_{B12} = (1 - \alpha_1)[A_1 \dot{h} - (1 - \gamma)Q_P] \qquad (10)$$

Basin #2, Surface Layer:

$$Q_{SB2} = Q_{S23} - Q_{S12} - (1 - \gamma)Q_P \qquad (11)$$

where:

Q_{SB2} = Flow rate, in Basin #2, from surface to bottom layer

Q_{S23} = Flow rate from the surface layer of Salem Sound into Basin #2, surface layer

Cooling water is assumed to be withdrawn solely from the surface layer of Basin #2. This rather unusual assumption is forced by the data available for model development: "intake temperature" is measured at a point 2 feet below the water surface, and ΔT across the plant is computed between this point and the discharge. Since the model is designed to use these ΔT values, it is necessary to assume intake water is withdrawn from the surface layer, at the "intake temperature", in order to maintain the proper heat balance:

Heat discharged = $Q_P\ T_{out}\ \rho\ c_P = Q_P(T_{in} + \Delta T)\rho\ c_P$.

Basin #2, Bottom Layer:

$$\frac{d}{dt}(V_{B2}) = Q_{B23} + Q_{SB2} - Q_{B12} \tag{12}$$

where:

V_{B2} = Volume of Basin #2, bottom layer

Q_{B23} = Flow rate from the bottom layer of Salem Sound into Basin #2, bottom layer

Employing Eqs. (11) and (10), and simplifying:

$$Q_{S23} + Q_{B23} = (A_1 + A_2)\,\dot{h} = Q_{23} = \text{total flow into harbor} \tag{13}$$

By analogy to Basin #1, bottom layer:

$$Q_{S23} = \alpha_2\,(A_1 + A_2)\dot{h}$$

$$Q_{B23} = (1 - \alpha_2)(A_1 + A_2)\dot{h} \tag{14}$$

where

$$\alpha_2 = b_2\left[\frac{h_S}{h_S + h_{B2}}\right] \tag{15}$$

3.2.2 Conservation of Energy

Basin #1, Surface Layer:

$$\frac{d}{dt}(E_{S1}) = \rho\, c_p[Q_{S12}(a_1\, T_{S2} + (1 - a_1)\, T_{S1}) + (1 - \gamma)Q_P\, T_{out}$$

$$- Q_{SB1}\,(a_2\, T_{S1} + (1 - a_2)\, T_{B1})] + (\phi_{S1} - \phi_{B1})\, A_1 \tag{16}$$

where:

E_{S1} = Total thermal energy in Basin #1, surface layer

ρ = Density of salt water $\simeq$ 64 lbm/ft^3

c_p = Heat capacity of salt water $\simeq$ 1 BTU/lbm °F

T_{S1} = Temperature of Basin #1, surface layer

T_{S2} = Temperature of Basin #2, surface layer

T_{B1} = Temperature of Basin #1, bottom layer

T_{out} = Plant discharge temperature

ϕ_{S1} = Net surface heat flux, Basin #1

ϕ_{B1} = Surface-bottom heat transfer, Basin #1

$$a_1 = \begin{cases} 1, & Q_{S12} > 0 \\ 0, & Q_{S12} \leq 0 \end{cases}$$

$$a_2 = \begin{cases} 1, & Q_{SB1} > 0 \\ 0, & Q_{Sb1} \leq 0 \end{cases}$$

The switches a_1, etc. ensure that the proper energy balance applies, under varying flow directions.

The net surface heat flux (ϕ_{S1}) into or out of the surface layer is computed separately from each basin using equations adapted from Harleman and Stolzenbach (1975); the equations are summarized in Appendix A. All heat fluxes are in units of BTU/ft^2-hr.

The conductive heat transfer between surface and bottom layers (ϕ_{B1}) is modeled as a linear function of the temperature difference:

$$\phi_{B1} = k\ (T_{S1} - T_{B1}) \tag{17}$$

The discharge temperature, T_{out}, is computed by:

$$T_{out} = T_{in} + \Delta T \tag{18}$$

In simulation of historical temperatures, measured (not simulated) ΔT values are used. T_{in} is modeled as a function of temperatures in the surface layer in Basin #2 (see below).

An expansion of the left-hand side yields:

$$\frac{d}{dt}\ (E_{S1}) = (\rho\ c_P\ h_S\ A_1)\ \frac{d}{dt}\ (T_{S1}) \tag{19}$$

Simplifying, one obtains the equation for the temperature of this cell:

$$\frac{d}{dt}\ (T_{S1}) = \frac{1}{h_S A_1}[Q_{S12}\ (a_1\ T_{S2} + (1 - a_1)\ T_{S1}) + (1 - \gamma)Q_P T_{out} - Q_{SB1}\ (a_2\ T_{S1} + (1 - a_2)\ T_{B1})] + \frac{\phi_{S1} - \phi_{B1}}{\rho\ c_P\ h_S} \tag{20}$$

<u>Basin #1, Bottom Layer</u>:

$$\frac{d}{dt}\ (E_{B1}) = \rho\ c_P\ [Q_{B12}\ (a_3\ T_{B2} + (1 - a_3)T_{B1}) + Q_{SB1}\ (a_2\ T_{S1} + (1 - a_2)T_{B1})] + \phi_{B1}\ A_1 \tag{21}$$

where:

E_{B1} = total thermal energy in Basin #1, bottom layer

T_{B2} = temperature of Basin #2, bottom layer

$$a_3 = \begin{cases} 1 , & Q_{B12} > 0 \\ 0 , & Q_{B12} \leq 0 \end{cases}$$

Expanding the left-hand side:

$$\frac{d}{dt}(E_{B1}) = \rho\, c_p\, A_1\, [h_{B1}\, \dot{T}_{B1} + T_{B1}\, \dot{h}_{B1}] \tag{22}$$

Recalling Eq. (6), Eq. (21) is re-arranged to yield:

$$\frac{d}{dt}(T_{B1}) = \frac{1}{A_1 h_{B1}} [Q_{B12}\, a_3\, (T_{B2} - T_{B1}) + Q_{SB1}\, a_2\, (T_{S1} - T_{B1})] + \frac{\phi_{B1}}{\rho\, c_p\, h_{B1}} \tag{23}$$

Basin #2, Surface Layer:

$$\frac{d}{dt}(E_{S2}) = \rho\, c_p\, [Q_{S23}(a_4\, T_{S3} + (1 - a_4) T_{S2}) - Q_{S12}\, (a_1\, T_{S2} + (1 - a_1)\, T_{S1}) - Q_P(\gamma\, T_{out} - T_{in}) - Q_{SB2}\, (a_5\, T_{S2} + (1 - a_5)\, T_{B2})] + (\phi_{S2} - \phi_{B2}) A_2 \tag{24}$$

where:

E_{S2} = Total thermal energy in Basin #2, surface layer

T_{S3} = Temperature of water in the surface layer of Salem Sound at the open boundary

ϕ_{S2} = Net surface heat flux, Basin #2

ϕ_{B2} = Surface-bottom heat flux, Basin #2

$$a_4 = \begin{cases} 1 , & Q_{S23} > 0 \\ 0 , & Q_{S23} \leq 0 \end{cases}$$

$$a_5 = \begin{cases} 1 , & Q_{SB2} > 0 \\ 0 , & Q_{SB2} \leq 0 \end{cases}$$

Intake temperature T_{in} is modeled as a function of surface layer temperature (T_{S2}) and of wind speed and direction:

$$T_{in} = T_{S2} + f_{wind}$$

Since T_{in} in this case is measured 2 feet below the surface, it can be realistically approximated by T_{S2}. The additional temperature increment due to wind is based on a hypothesis that wind of the right magnitude and direction will blow the plume in towards the intake. This hypothesis is partially supported by wind and temperature data, and by the fairly successful subjective-intuitive model (Kenison and Galli, 1975) using this hypothesis. This experience suggests that the temperature increment increases in a high-order way with wind speed. Temperature increase also appears to reach a maximum around a particular wind direction. To allow enough vari-

ability to reproduce these relationships, the wind function used is:

$$f_{wind} = [g_1 + g_2\ WS + g_3\ WS^2 + g_4\ WS^3][g_8 + g_5 \exp -(\frac{g_6 - WD}{g_7})^2] \quad (25)$$

where:

WS = wind speed in miles/hour

WD = wind direction in °North

g_i = parameters of wind function.

The open-boundary condition T_{S3} is modeled as follows:

1) Ebb Tide ($Q_{S23} \leq 0$)

$$T_{S3}(n) = T_{S2}(n)$$

2) Flood Tide ($Q_{S23} > 0$)

$$T_{S3}(n) = T_{S2,low} - C_1(T_{S2,low} - T_{S,sound})(\frac{n - n_{low}}{6.2}) \quad (26)$$

where:

$T_{S2,low}$ = T_{S2} at most recent low tide

n_{low} = time of most recent low tide

$T_{S,sound}$ = background surface temperature of Salem Sound (unaffected by plant)

C_1 = fraction of initial temperature difference over which T_{S3} will vary during flood tide

That is, on ebb tide the temperature at the boundary equals the temperature of exiting water. On flood tide, the boundary temperature changes linearly from hottest (at low tide) to background (at

high tide), if $C_1 = 1$. If $C_1 < 1$, boundary temperature will not drop all the way to background. For historical simulation runs, daily average values of $T_{S,sound}$ are obtained from interpolation of bi-weekly surface temperature measurements.

Re-arranging Eq. (24), as was done above for the surface, Basin #1, one obtains:

$$\frac{d}{dt}(T_{S2}) = \frac{1}{h_S A_2}\left[Q_{S23}\,(a_4\,T_{S3} + (1 - a_4)T_{S2}) - Q_{S12}\,(a_1\,T_{S2} + (1 - a_1)\,T_{S1}) - Q_p(\gamma T_{out} - T_{in}) - Q_{SB2}\,(a_5\,T_{S2} + (1 - a_5)T_{B2}\right] + \frac{\phi_{S2} - \phi_{B2}}{\rho\, c_p\, h_S} \qquad (27)$$

Basin #2, Bottom Layer:

$$\frac{d}{dt}(E_{B2}) = \rho\, c_p\left[Q_{B23}\,(a_6\,T_{B3} + (1 - a_6)T_{B2}) + Q_{SB2}\,(a_5\,T_{S2} + (1 - a_5)T_{B2}) - Q_{B12}\,(a_3\,T_{B2} + (1 - a_3)\,T_{B1})\right] + \phi_{B2}A_2 \qquad (28)$$

where:

E_{B2} = total thermal energy in Basin #2, bottom layer

T_{B3} = temperature of bottom layer of Salem Sound at open boundary

$$a_6 = \begin{cases} 1, & Q_{B23} > 0 \\ 0, & Q_{B23} \leq 0 \end{cases}$$

Open-boundary temperature T_{B3} is modeled analogously to T_{S3}:

$$\underline{\text{Ebb Tide}} \quad (Q_{B23} \leq 0) - \tag{29}$$

$$T_{B3}(n) = T_{B2}(n)$$

$$\underline{\text{Flood Tide}} \quad (Q_{B23} > 0) -$$

$$T_{B3}(n) = T_{B2,low} - C_2(T_{B2,low} - T_{B,sound})\left(\frac{n - n_{low}}{6.2}\right)$$

$T_{B,sound}$ is assumed to be 1.5° F less than $T_{S,sound}$ for any day.

Expanding the left-hand side of Eq. (28), and recalling Eq. (12), Eq. (28) simplifies to:

$$\frac{d}{dt}(T_{B2}) = \frac{1}{h_{B2}A_2}\left[Q_{B23}\, a_6\, (T_{B3} - T_{B2}) + Q_{SB2}\, a_5\, (T_{S2} - T_{B2}) + Q_{B12}\,(1 - a_3)(T_{B2} - T_{B1})\right] + \frac{\phi_{B1}}{\rho\, c_p\, h_{B2}} \tag{30}$$

This completes the development of the proposed basin-type model. Tables 3-2 and 3-3 summarize its basic elements. The harbor is idealized as a rectangular, 2-basin, 2-layer system; water is assumed well-mixed in each cell. The surface layer is assumed of constant depth; the bottom layer rises and falls with the tide. Tidal levels are known a priori from published tide tables; these levels "drive" the inter-cell flows of water. Surface heat flux includes the processes of short- and long-wave absorption, reflection, and radiation; evaporation; and conduction. Special assumptions are made about open-boundary conditions, and about re-circulation of power plant discharge.

Table 3-2

Flow Equations for Two-Basin, Two-Layer Model

$$Q_{S12} = \alpha_1[A_1 \dot{h} - (1 - \gamma)Q_P]$$

$$Q_{B12} = (1 - \alpha_1)[A_1 \dot{h} - (1 - \gamma)Q_P]$$

$$Q_{SB1} = Q_{S12} + (1 - \gamma)Q_P$$

$$Q_{S23} = \alpha_2 (A_1 + A_2)\dot{h}$$

$$Q_{B23} = (1 - \alpha_2)(A_1 + A_2)\dot{h}$$

$$Q_{SB2} = Q_{S23} - Q_{S12} - (1 - \gamma)Q_P$$

Table 3-3

Temperature Equations for Two-Basin, Two Layer Model

$$\frac{d}{dt}(T_{S1}) = \frac{1}{h_S A_1}\left[Q_{S12}\,(a_1\,T_{S2} + (1 - a_1)T_{S1}) + (1 - \gamma)Q_P\,T_{out} - Q_{SB1}\,(a_2\,T_{S1} + (1 - a_2)T_{B1})\right] + \frac{(\phi_{S1} - \phi_{B1})}{\rho\,c_P\,h_S}$$

$$\frac{d}{dt}(T_{B1}) = \frac{1}{h_{B1} A_1}\left[Q_{B12}\,a_3\,(T_{B2} - T_{B1}) + Q_{SB1}\,a_2(T_{S1} - T_{B1})\right] + \frac{\phi_{B1}}{\rho\,c_P\,h_{B1}}$$

$$\frac{d}{dt}(T_{S2}) = \frac{1}{h_S A_2}\left[Q_{S23}\,(a_4\,T_{S3} + (1 - a_4)T_S 2) - Q_{S12}\,(a_1\,T_{S2} + (1 - a_1)T_{S1}) - Q_P\,(\gamma\,T_{out} - T_{in}) - Q_{SB2}\,(a_5\,T_{S2} + (1 - a_5)T_{B2})\right] + \frac{(\phi_{S2} - \phi_{B2})}{\rho\,c_P\,h_S}$$

$$\frac{d}{dt}(T_{B2}) = \frac{1}{h_{B2} A_2}\left[Q_{B23}\,a_6\,(T_{B3} - T_{B2}) + Q_{SB2}\,a_5\,(T_{S2} - T_{B2}) + Q_{B12}\,(1 - a_3)(T_{B2} - T_{B1})\right] + \frac{\phi_{B1}}{\rho\,c_P\,h_{B2}}$$

3.3 The Model in State-Space Form

To employ parameter-estimation techniques, the model must be transformed into stochastic state-space form. The steps in this transformation are executed below.

First, the model is discretized. Since a basin-type model is inherently discretized in space, it remains only to discretize in time the equations of Tables 3-2 and 3-3. The following discretizations are used:

Tide:

$$\frac{d}{dt}(h)\Big|_n \simeq \frac{h(n+1) - h(n-1)}{2(\Delta t)}$$

Temperature:

$$\frac{d}{dt}(T)\Big|_n \simeq \frac{T(n+1) - T(n)}{\Delta t}$$

Second, the appropriate state-variables are identified. In this case, there are six state-variables: the volume-averaged temperature of each of the four cells, plus the two low-tide open-boundary conditions from the most recent low tide (which influence future values of the other states via flood-tide open boundary conditions). Note that the inter-cell flows are considered exogenous inputs, not states. These flows can be computed directly from the tidal levels and plant discharge, known a priori.

Third, the model equations are transformed to explicit, linear, recursive equations for each state variable. Since the net surface heat flux is non-linear with surface temperature, a linearization is

performed (Appendix A).

Fourth, a model of the observations as a function of the states is developed. The only observations in this case are hourly plant intake temperatures (measured two feet below the surface). The observation equation is $T_{in} = T_{S2} + f_{wind}$.

Last, a stochastic component is added to the heretofore deterministic model. The random variables w_i and v_i, added to the model equations, are assumed to be zero-mean and uncorrelated in time.

The governing equations from Tables 3-3 and 3-4 are transformed as above into state-space, white process form. In vector-matrix form, the proposed model is:

$$\underline{x}(n+1) = \underline{\underline{F}}\,(\underline{u}(n), \underline{\alpha}, n)\,\underline{x}(n) + \underline{b}(\underline{u}(n), \underline{\alpha}, n) + \underline{w}(n)$$

$$z(n) = x_3(n) + f_{wind}(\underline{u}(n), \underline{\alpha}) + v(n)$$

$$\underline{x}(n) = \begin{bmatrix} T_{S1}(n) \\ T_{B1} \\ T_{S2} \\ T_{B2} \\ T_{S2,low}(n) \\ T_{B2,low}(n) \end{bmatrix} \qquad \underline{u}(n) = \begin{bmatrix} h(n) \\ Q_p(n) \\ WS(n) \\ WD(n) \\ T_{air}(n) \\ T_{dew}(n) \\ c(n) \\ T_{sound}(n) \\ T(n) \end{bmatrix}$$

$\underline{\alpha}$ = vector of unknown parameters (see Table 4-1 for listing)

$z(n) = T_{in,measured}(n)$

$\underline{\underline{F}}(\ )$ = state transition matrix

$\underline{b}(\ )$ = vector function of exogenous inputs

$\underline{w}(n)$, $v(n)$ = white noise processes

The model is now in a form allowing application of the estimation techniques described in Chapter Two. In this form, several noteworthy characteristics of the model are evident. The model is linear in the states, though non-linear in the inputs; thus, it is amenable to filtering. Model coefficients are time-varying; thus, simplifying assumptions about a "steady-state filter" are not applicable. The model is highly unobservable: the dimension of the measurement vector is 1, while the dimension of the state-vector is 6. Thus, accurate estimation of the states is difficult.

CHAPTER FOUR

PARAMETER ESTIMATION AND MODEL EVALUATION

The proposed structure contains thirty-three unknown or poorly known parameters, summarized in Table 4-1. In this chapter full information maximum-likelihood (FIML) estimation is employed to obtain optimal estimates of these parameters. Section 4.1 presents initial parameter values and their rationale. Section 4.2 presents the steps of the estimation process and the resulting parameter estimates. The data base for parameter estimation is described in Section 4.3. Results of model performance tests are presented in Section 4.4.
In Section 4.5 an evaluation of the model is presented. All estimation, testing, and plotting is done using GPSIE.

4.1 Initial Parameter Values

Initial parameter estimates are listed in the first column of Table 4-2. The rationale for these initial values is given below:

$g_1 - g_8$: Estimated so that f_{wind} corresponds to subjective wind function in Kenison and Galli (1975)

$F_1 - F_3$: From Harleman and Stolzenbach (1975)

F_2, F_4, F_5, F_7: From Harleman and Stolzenbach (1975), divided by 24 to yield hourly values

$F_6 - F_8$: Initially set to 1, to be equivalent to Harleman and Stolzenbach (1975)

$b_1 - b_2$: Subjectively chosen to represent a vertical velocity profile at basin interfaces.

TABLE 4-1

PARAMETERS TO BE ESTIMATED

Parameter	Description
$g_1 - g_8$	Parameters of wind function f_{wind}
$F_1 - F_8$	Parameters of surface heat flux equations
$b_1 - b_2$	Velocity profile factors
$C_1 - C_2$	Flood-tide heat return factors for open boundary condition
$\gamma_1 - \gamma_2$	Plume re-circulation factors
$A_1 - A_2$	Basin surface areas
h_S	Surface layer thickness
$h_{B1,min}$ —	Minimum depth of bottom layers
$h_{B2,min}$	
k	Surface-bottom heat exchange coefficient
σ^2_{S1}, σ^2_{B1}, σ^2_{S2}, σ^2_{B2}	Variance of model noise
σ^2_Z	Variance of measurement noise

$C_1 - C_2$: Subjectively chosen to represent maximum heat return to harbor during flood tide.

γ_1: Subjectively chosen to represent full re-circulation of discharge plume into Basin #2 at peak ebb tide.

γ_2: Subjectively chosen to represent zero plume re-circulation during flood tide.

$A_1 - A_2$: Estimated from harbor measurements

h_s: Estimated from temperature profiles

$h_{B1,min}$,

$h_{B2,min}$: Estimated from harbor hydrography

k: Subjectively chosen

σ_{S1}^2, σ_{B1}^2

σ_{S2}^2, σ_{B2}^2: Subjective estimates of model accuracy

σ_z^2: Subjective estimate of measurement accuracy

The model noise statistics $\sigma_{S1}^2 - \sigma_{B2}^2$ represent the first four diagonal elements of the covariance matrix $\underline{Q}$. The last two diagonal elements, $\sigma_{S2,low}^2$ and $\sigma_{B2,low}^2$, are assumed equal to σ_{S2}^2 and σ_{B2}^2, respectively, and are not estimated separately. This assumption is made because of the close physical relation between T_{S2} and $T_{S2,low}$, being identically equal once every tidal cycle (and similarly, in the bottom layer). Off-diagonal elements of $\underline{Q}$ (i.e., cross-covariances of model noise) are assumed zero.

4.2 The Estimation Process

Parameter estimation is done in two phases: Phase I - Preliminary Estimation, and Phase II - Global Optimal Estimation. Phase I provides a coarse and somewhat subjective refinement of selected initial parameter estimates. The results of Phase I provide initial conditions for the global optimization of all parameters in Phase II.

Each phase of the estimation process involves several steps, presented below. In the discussion, a distinction is made between structural parameters and noise parameters. Structural parameters are those in the state and measurement equations. There are 28 unknown structural parameters in the present problem (the first 28 variables in Table 4-1). Noise parameters are those defining the covariances of the model and measurement noise; there are 5 unknown noise parameters in the present problem (see Table 4-1).

Phase I includes the following steps:

(1) Powell search for FIML estimates of g_{1-8}, the parameters of f_{wind}. The wind function parameters are the least well-known of the parameters to be estimated; thus, the preliminary estimation begins by refining these values.

(2) Manual search of selected structural parameters for FIML estimates within realistic bounds. This step uses the modeler's judgment to bound a preliminary manual search for improved estimates within realistic limits. Parameters appearing to offer the greatest potential for model improvement are manually optimized. Rough

bounds on what is realistic are drawn from data on Salem Harbor and engineering experience with thermal discharges.

(3) Manual search for FIML estimates of noise parameters σ_i. Using the above estimates of structural parameters, revised estimates of the noise statistics σ_i are developed via manual search.

Step 3 concludes the preliminary estimation. The preliminary parameter estimates are the revised wind parameters, other revised structural parameters, the revised noise statistics, and the initial estimates of all other unrevised parameters. These estimates form the starting point for the global estimation.

Part II of the process includes the following steps:

(4) Powell search for FIML estimates of all structural parameters. The 28 structural parameters are estimated simultaneously, using a Powell search to find the global FIML estimate. Noise statistics are not included in the Powell search because of potential problems if the search explores negative values for the covariances. (A bounded search is not possible using GPSIE). Cost of estimation is approximately $300.

(5) Manual search for noise statistics with improved S. At the global FIML estimates from the previous step, S is much less than E[S], as shown in Table 4-2. (The S statistic is discussed in Section 2.2). To increase S, the noise statistics are manually adjusted in this step until S is approximately equal to E[S].

(6) Final Powell search for FIML estimates of structural parameters. The revised noise statistics are significantly different from their previous values (at the end of step 3). To ensure parameter estimation with the proper noise statistics, all structural parameters are re-estimated in this step using the revised noise statistics. Cost of the estimation is approximately $500. The S value for this estimation is almost within $2\sigma_S$ of its expected value; thus the noise statistics are not decreased further. The estimation is checked to see if increasing the noise statistics (towards their previous values) improves the log-likelihood. The check indicates that the noise statistics do not need to be changed further, and the estimation process is ended (see Appendix D). The results of this step are the final parameter estimates.

The step-wise evolution of the parameter estimates is summarized in Table 4-2. These results are discussed in Section 4.5.

TABLE 4-2:

PARAMETER ESTIMATES AT STEPS OF THE ESTIMATION PROCESS

PARAMETER	PHASE I - PRELIMINARY				PHASE II - FINAL		
	INITIAL ESTIMATE	POWELL/FIML ESTIMATE OF f_{wind}	MANUAL SEARCH OF STRUCTURAL PARAMETERS (FIML)	MANUAL SEARCH OF NOISE PARAMETERS (FIML)	POWELL/FIML ESTIMATE OF STRUCTURAL PARAMETERS	MANUAL SEARCH OF NOISE PARAMETERS (S)	POWELL/FIML ESTIMATE OF STRUCTURAL PARAMETERS
g_1	0	-.707			.0409		2.53
g_2	0	0			.0594		-.0518
g_3	.015	.015			.0157		.0145
g_4	-.0005	-.00054			-.00045		-.00041
g_5	2.	1.9			2.76		3.47
g_6	145.	133.			155.		-116.
g_7	40.	36.6			298.		1510
g_8	-1.	-.8			-1.4		-1.5
F_1	.65		.95		1.88		1.46
F_2	4.34				7.34		2.40
F_3	.17				11.8		8.8
F_4	6.64				6.10		7180.
F_5	.584		2.0		18.5		5.54
F_6	1.0		1.2		-4.11		-3.43
F_7	1.66				218.		210.
F_8	1.				.518		.378
b_1	1.		.8		9.03		3.16
b_2	1.		.8		5.23		2.94
C_1	1.				6.87		.105
C_2	1.				1.64		1.01
γ_1	1.		.5		- .115		-14.4
γ_2	0				-3.51		-11.8
A_1	20×10^6				19×10^6		4×10^6

TABLE 4-2 (continued)

PARAMETER ESTIMATES AT STEPS OF THE ESTIMATION PROCESS

	PHASE I - PRELIMINARY				PHASE II - FINAL		
PARAM-ETER	INITIAL ESTIMATE	POWELL/FIML ESTIMATE OF f_{wind}	MANUAL SEARCH OF STRUCTURAL PARAMETERS (FIML)	MANUAL SEARCH OF NOISE PARAMETERS (FIML)	POWELL/FIML ESTIMATE OF STRUCTURAL PARAMETERS	MANUAL SEARCH OF NOISE PARAMETERS (S)	POWELL/FIML ESTIMATE OF STRUCTURAL PARAMETERS
A_2	12×10^6		15×10^6		15.9×10^6		8×10^6
h_s	2.		6.		6.82		9.83
$h_{B1,min}$	8.				5.16		14.5
$h_{B2,min}$	8.				4.19		3.6
k	1.				3.88		2.59
σ^2_{S1}	1.			5.		3.	
σ^2_{B1}	1.			4.		2.	
σ^2_{S2}	1.			20.		1.5	
σ^2_{B2}	1.			6.		2.	
σ^2_z	.04			.1		.04	
Log-Likelihood				-196.3	-170.2	-109.3	-87.0
S		(NOT RE-CORDED)		-	13.	92.5	40.4
E[S]				-	63.	92.	63.
σ_S				-	11.2	13.5	11.2

4.3 Data Base for Estimation and Testing

Model development and testing is done on data from late spring and summer of 1974. This season is chosen because it is of greatest concern relative to water temperature control. Developing the model strictly for late spring and summer maximizes its applicability to the dominant hydrothermal processes of this season. The study is confined to 1974 data because this is the only year for which comprehensive and consistent data is available (though further data is being collected).

During late spring and summer of 1974 there are four periods in which complete, uninterrupted data are available. These data periods are (to the hour): 2100, May 17 to 1400, June 13; 1700, June 25 to 1000, July 22; 2100, July 29 to 1500, August 21; 2400, August 23 to 2400, September 20. Parameter estimation is done on a small subset of this data. Model testing is done on the complete data base.

Selecting the base period length for parameter estimation involves a trade-off between uncertainty and cost. Since little prior experience exists on FIML estimation for this type of modeling problem, the base periods for Phases I and II are chosen fairly subjectively. The length of the base period for global estimation is chosen so that the number of data points is approximately four times the number of unknowns (dimension of $\underline{\alpha}$). A longer base period may improve the parameter estimates; however, this relationship is not examined in this study. Since the estimations in Phase I involve fewer parameters and less numerical

detail than Phase II (see below), Phase I may employ a longer base period. The following base periods are used:

Phase I: 294 hours (12 days) 2100, 7/29 - 0300, 8/10

Phase II: 96 hours (4 days) 2100, 7/29 - 2000, 8/2

These dates are chosen to be roughly characteristic of mid-summer weather, water and generation conditions. For maximum comparability, both base periods are chosen to begin with the start of a data period.

4.4 Model Performance

Model performance is evaluated for two reasons: first, to evaluate whether the model meets the accuracy criterion of the original model development problem; and second, to assess the effectiveness of the final parameter estimation process. Visual and quantitative indicators of model performance are computed to provide data for these evaluations.

The preliminary model (using the parameter estimates in Columns 1-4 of Table 4-2) and the final model (using the parameter estimates in Columns 6-7 of Table 4-2) are tested. For ease of comparison, the noise statistics in the preliminary model are equated to the noise statistics of the final model. The identical noise covariances ensure that any differences in likelihood or S-statistic are due only to differences in residuals from each model.

Figures 4-1 through 4-3 allow visual assessment of final model behavior. These plots show unfiltered 24-hour predictions of intake temperatures, for three days (one month prior to the base period). The measurements and the confidence bounds of the predictions are plotted concurrently. For comparison, similar plots from the preliminary model are shown in Figures 4-4 through 4-6. These results are discussed in Section 4.5.

A variety of measures of model performance are useful (Section 2.2):

ξ - The full-information likelihood

T - The percent of daily peak temperature predictions within 1°F

FIGURE 4-1

PREDICTED INTAKE TEMPERATURES FROM FINAL MODEL (6/29 - 6-30/74)

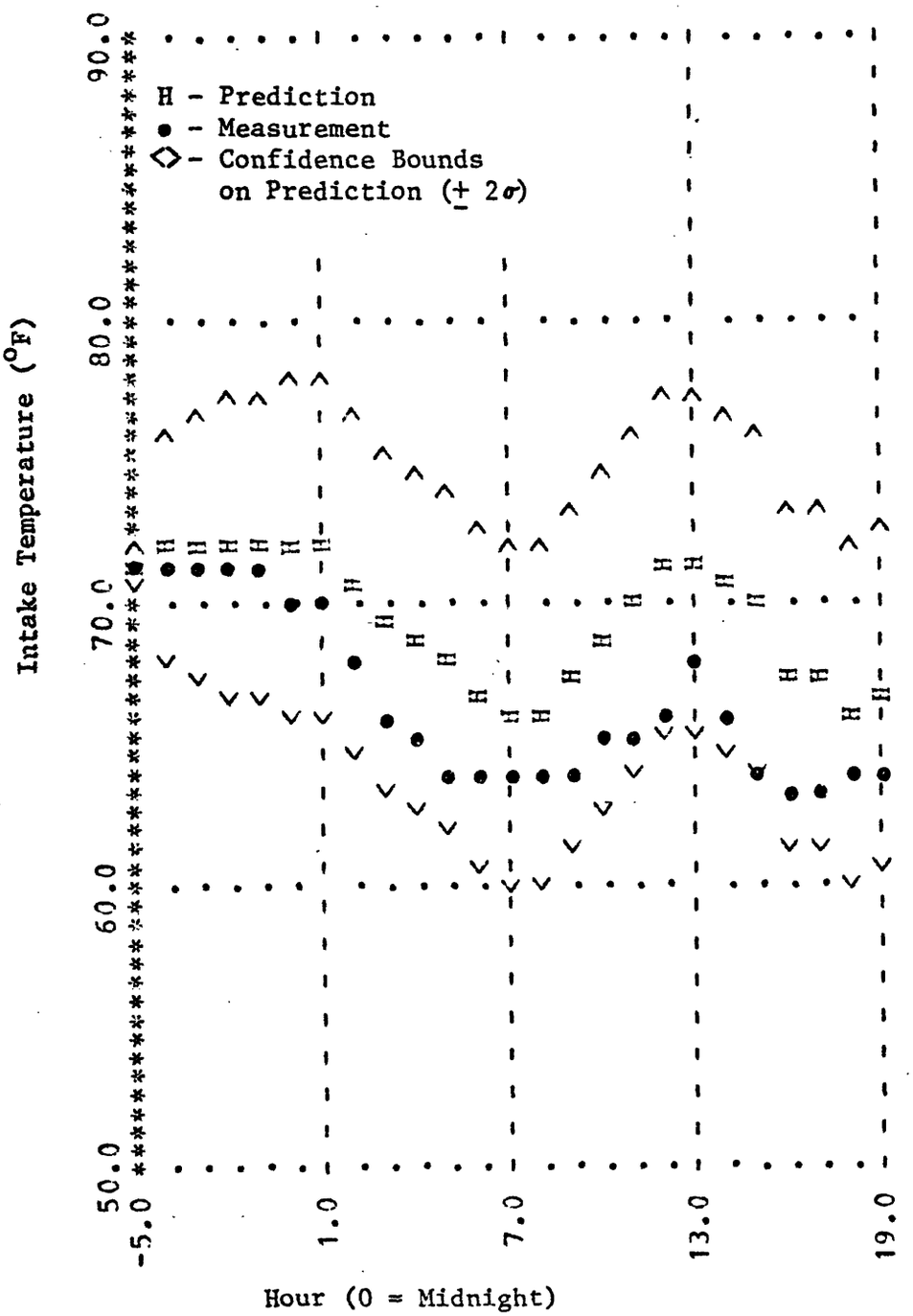

FIGURE 4-2

PREDICTED INTAKE TEMPERATURES FROM FINAL MODEL 6/30 - 6/31/74

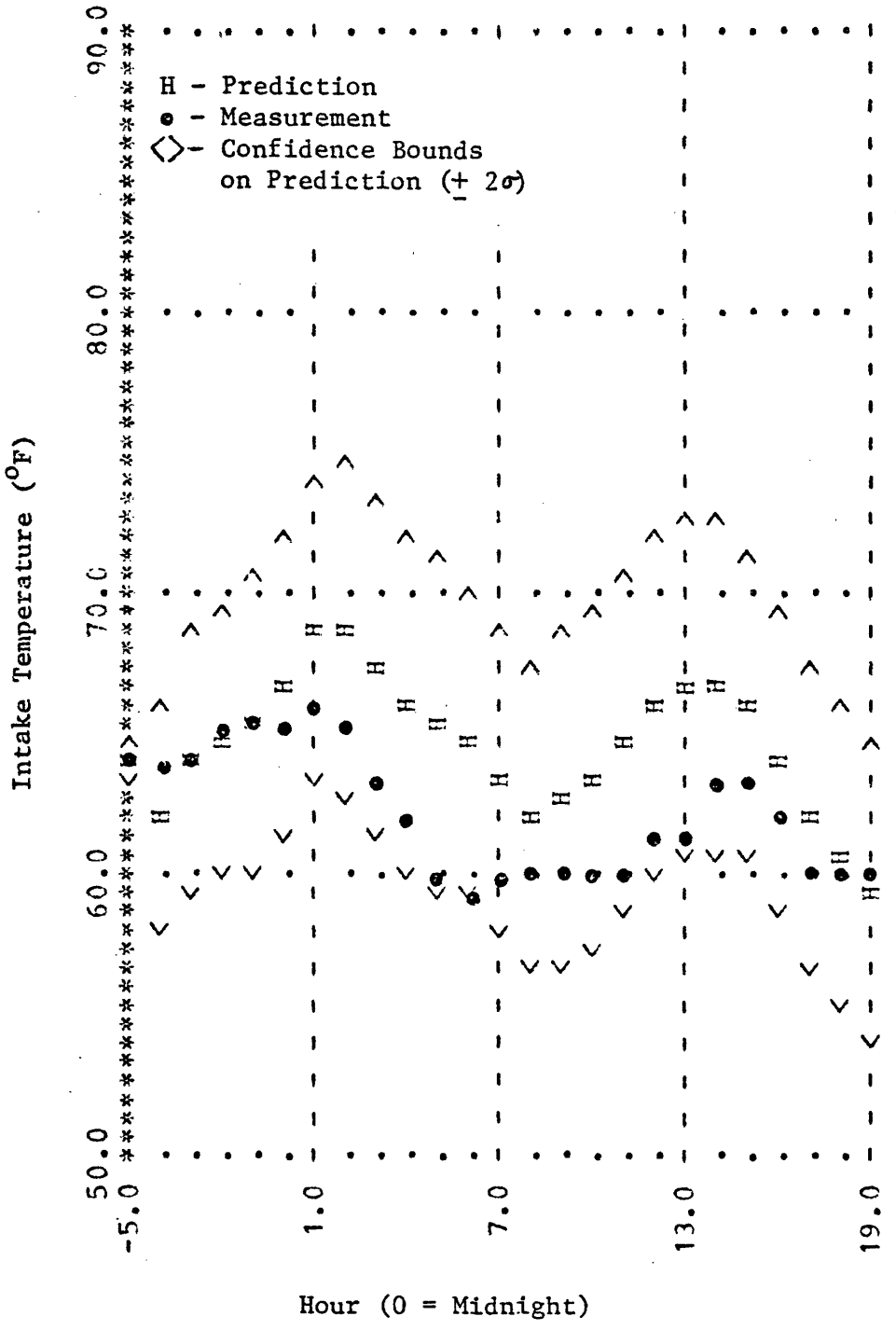

FIGURE 4-3

PREDICTED INTAKE TEMPERATURES FROM FINAL MODEL 6/31 - 7/1/74

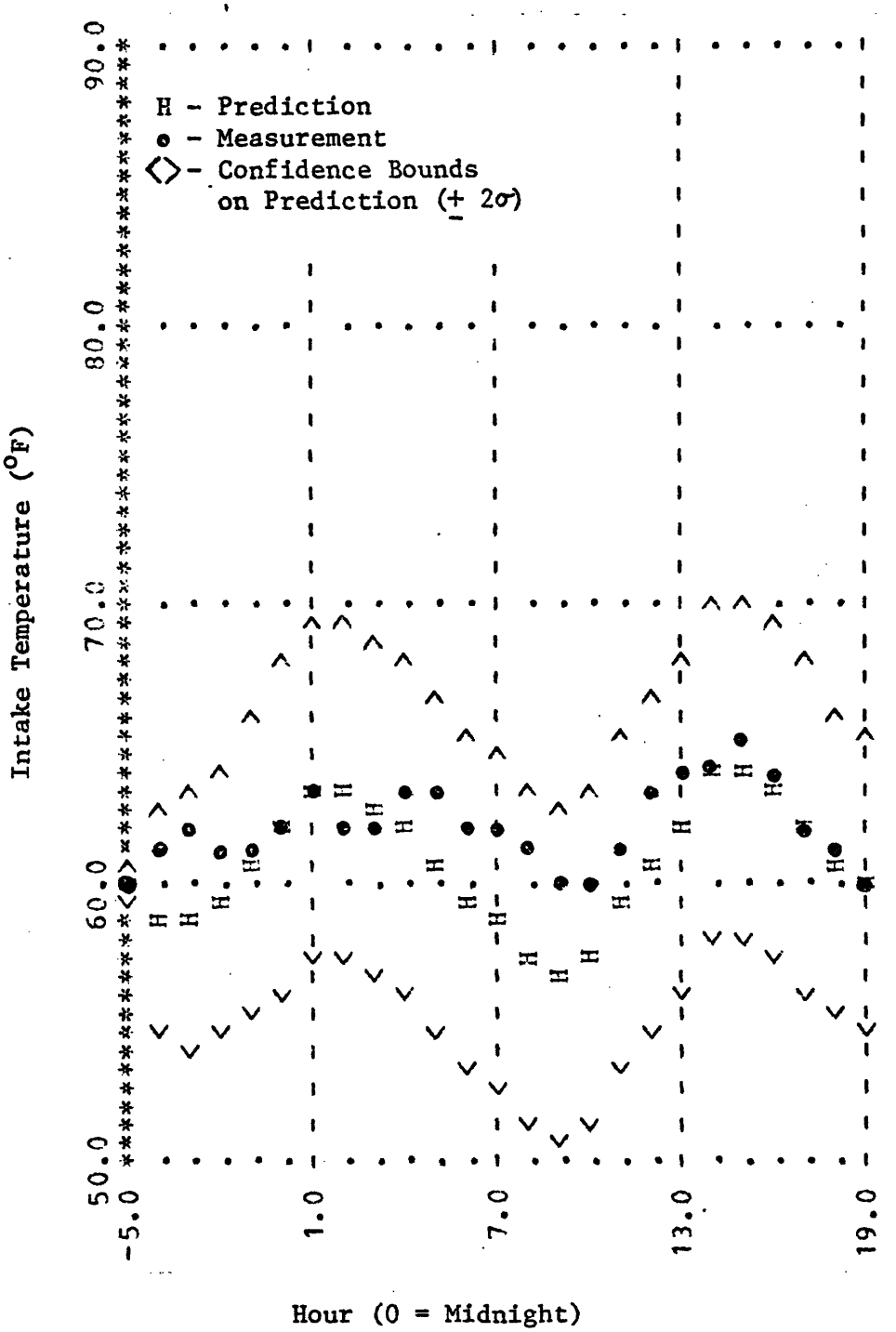

FIGURE 4-4

PREDICTED INTAKE TEMPERATURES FROM PRELIMINARY MODEL (6/29-6/30/74)

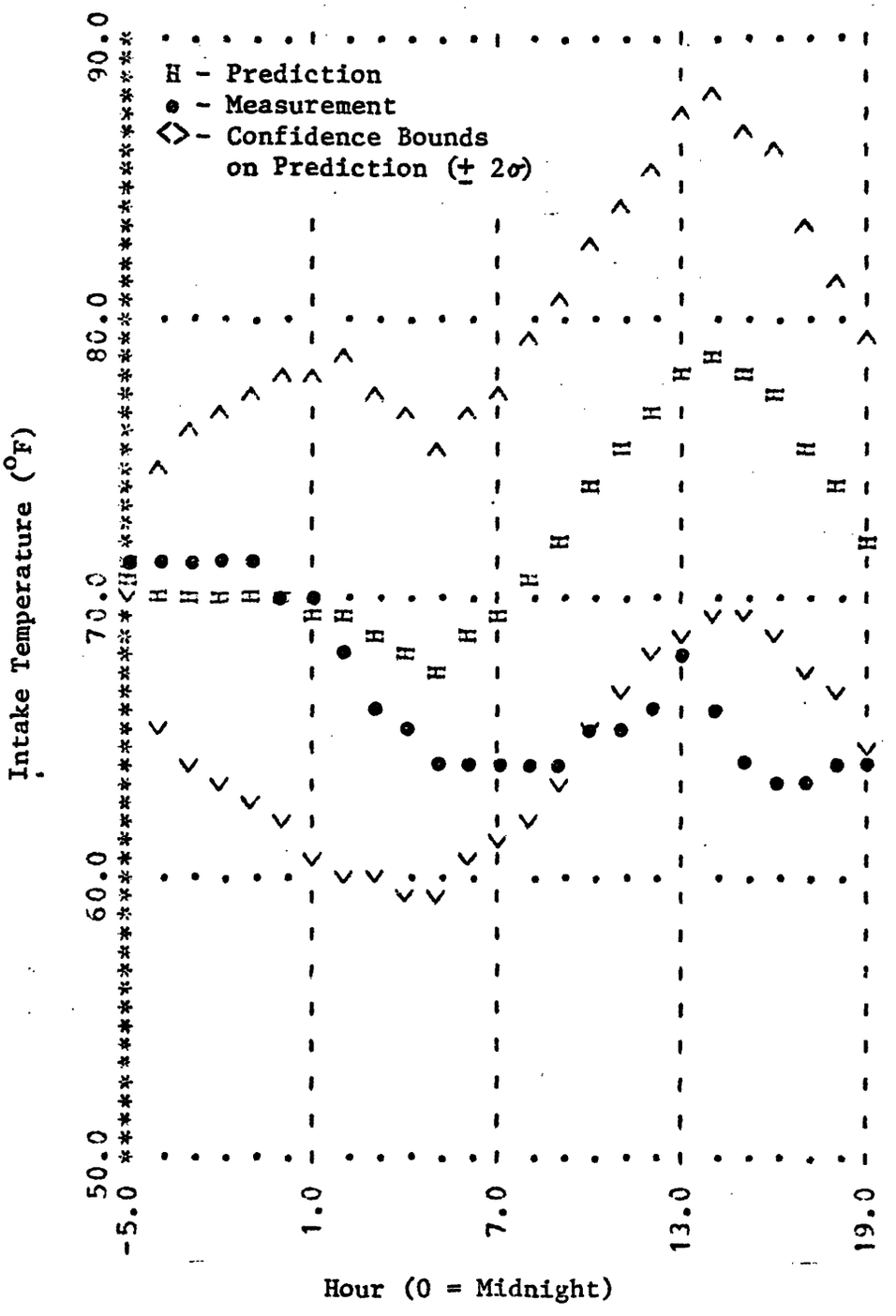

FIGURE 4-5

PREDICTED INTAKE TEMPERATURES FROM PRELIMINARY MODEL (6/30-6/31/74)

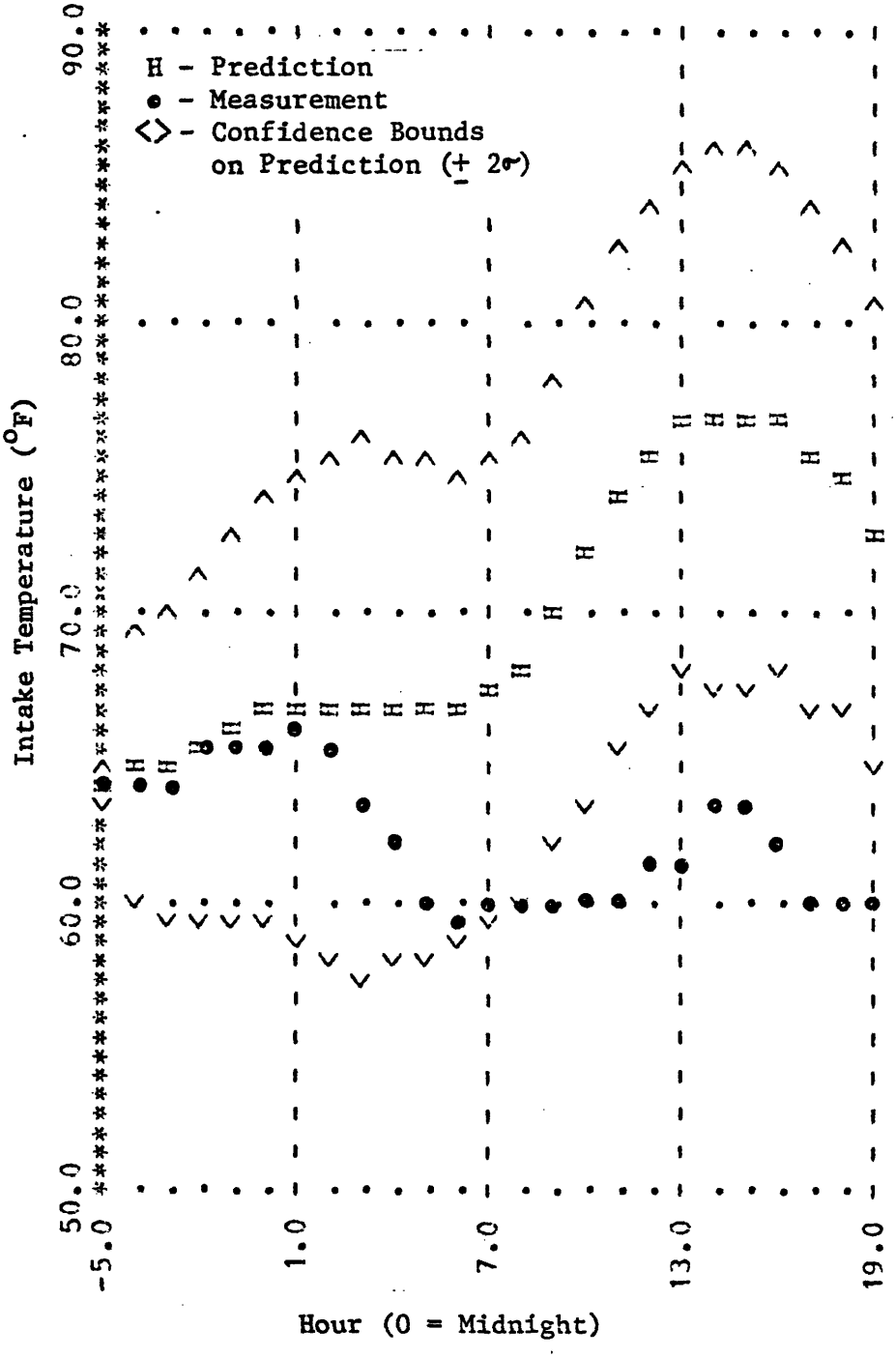

FIGURE 4-6

PREDICTED INTAKE TEMPERATURES FROM PRELIMINARY MODEL (6/31-7/1/74)

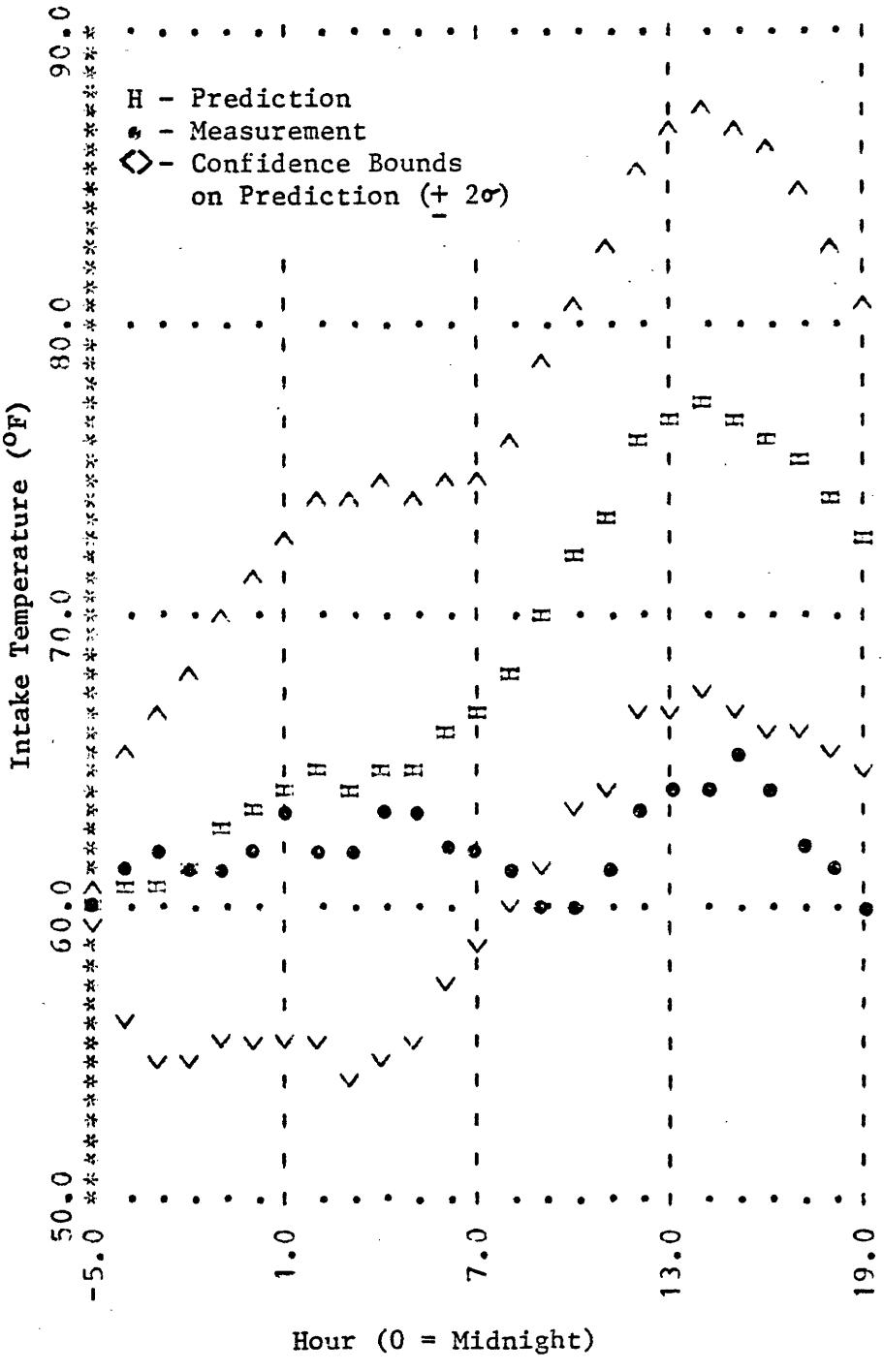

of measured peak. (Original accuracy criterion specified in these terms).

D - The mean-square error in daily peak temperature predictions.

M - The mean-square error in 24-hour temperature predictions.

S - The sum-of-squares of normalized measurement residuals.

$\underline{\underline{P}}(a)$- The whiteness-test matrix for lag a.

σ_z^2 - The covariance of a 24-hour prediction.

The final model is run for the four data periods representing late-spring and summer of 1974, and model performance is computed using the above measures. For comparison, performance of the preliminary model is also computed.

The results of this model performance evaluation are presented in Table 4-3. (Note that the T value is computed to show percent of daily peak intake temperature predictions within 1°F, 2°F, and 3°F of observed temperatures.)

TABLE 4-3: RESULTS OF MODEL PERFORMANCE TESTS

	5/17 - 6/13		6/25 - 7/22		7/29 - 8/21		8/23 - 9/20		BASE PERIOD 7/29-8/2	
	FINAL	PRELIM.	FINAL	PRELIM.	FINAL	PRELIM.	FINAL	PRELIM.	FINAL	PRELIM.
E[S]	609		609		514		640		63	
σ_S	34.9		34.9		32.1		35.8		11.2	
Log-likelihood										
ξ	-713.2	-646.9	-662.3	-691.9	-514.8	-568.4	-609.9	-650.3	-87.0	-105.9
S	614	254	503	348	321	252	354	211	40.4	56.2
T										
1°	8%	20%	16%	4%	5%	5%	27%	27%	--	--
2°	12%	40%	24%	8%	28%	5%	54%	35%		
3°	24%	52%	36%	20%	38%	19%	73%	54%		
D	60.39	27.84	24.35	70.97	18.53	40.1	10.16	13.13	--	--
($\sqrt{D}$)	(7.71)	(5.27)	(4.93)	(8.42)	(4.30)	(6.33)	(3.19)	(3.62)		
M	98.4	17.5	19.4	38.6	16.4	26.9	10.1	7.7	10.7	27.3
($\sqrt{M}$)	(9.92)	(4.18)	(4.40)	(6.21)	(4.05)	(5.19)	(3.18)	(2.77)	(3.27)	(5.22)
Whiteness									--	--
P(0)	- .8	-10.8	- 3.9	- 8.2	- 6.8	- 8.9	- 8.7	-12.7		
P(1)	16.7	5.2	12.3	8.9	7.1	5.4	7.1	2.8		
P(2)	11.2	3.0	5.8	5.5	2.8	3.7	2.8	0.9		
P(3)	6.3	1.6	0.6	3.7	0.3	2.4	0.2	0.4		
σ_z^2 (24|1)	--	--	8.84 (for 6/29--6/30)	14.34	--	--	--	--	--	--

4.5 Model Evaluation

The performance tests provide a rich background for evaluating the model and estimation techniques used in this study. Since the study objectives and methodology are new to water quality modeling, it is not surprising that several unlikely results are observed for which there is no definite explanation. From the present analyses potential explanations may be suggested but not confirmed. In several cases, questions must remain unanswered, awaiting further study.

4.5.1 Discussion of Parameter Estimates

The structural parameter values developed in the preliminary estimation are relatively close to their initial values. The Powell-FIML estimation of wind function parameters yields only a slight revision in values. A manual search of other structural parameters is deliberately kept within realistic bounds.

The re-estimated noise statistics at the end of Phase I (column 4 of Table 4-2) are much larger than their initial values or their final values. A possible explanation is that the much longer Phase I base period requires larger noise convariances to explain the data. Note that re-estimation of the noise statistics in Phase II, with a much shorter base period, produces much smaller convariances.

In the global estimation phase, several structural parameters assume unrealistic values. Examples from the final parameter estimates are:

A_1, A_2: Final values total only 1/3 of the actual harbor surface area,

F_7, F_4: The coefficients of ϕ_{br} (radiative heat loss) and ϕ'_{br} are too large by factors of 100 and 1000, respectively.

F_1 : Cannot be greater than 1; otherwise, on very cloudy days insolent radiation is negative.

F_6 : Cannot be negative; otherwise, ϕ_{br} will decrease with increasing surface temperature.

γ_1, γ_2: Cannot be negative; otherwise, there will be "negative recirculation" of discharge water from intake to discharge.

b_1, b_2: Values greater than 2 suggest unrealistically high flow velocities in the surface layer.

h_S : Surface layers deeper than 6 feet are not observed in Salem Harbor.

$h_{B1,min}, h_{B2,min}$: Basin #2 should be <u>deeper</u> than basin #1, to follow the harbor profile.

The unrealistic final parameter estimates suggest that there are significant structural flaws in the model. Observations of model behavior with realistic parameter values (eg., Figures 4-4 - 4-6) show that it consistently predicts erroneously high temperatures. The global, FIML-Powell parameter estimates correct this behavior (eg., Figure 4-1 - 4-3), but in so doing are forced to assume unrealistic values. In effect, the unrealistic parameter estimates compensate for an unrealistic model structure.

Unrealistic parameter estimates do not invalidate the model, but they do interfere with a physical interpretation of the model. In the present situation, it is best to abandon physical concepts, and to view the model instead as an abstract mathematical structure describing a time-series of data. By this view, the parameters are merely coefficients in the model, with no physical significance and no a priori bounds on their values.

Although both the first and second global estimations produce unrealistic values, the second contains more unrealistic values than the first. This result suggests that the estimation is sensitive to the size of the noise statistics used. Inspection of the log-likelihood equation,

$$2\xi(n) = 2\xi(n-1) - k\ell n\, 2\pi - \ell n[\det \underline{\underline{\Sigma}}_Z(n|n-1)] - \delta_z'(n)\underline{\underline{\Sigma}}_Z^{-1}(n|n-1)\underline{\delta}_Z(n)$$

helps to explain this result. As the noise covariances decrease, $\underline{\underline{\Sigma}}_Z$ decreases; hence, the last term in the likelihood equation becomes larger. Thus, the likelihood is increasingly sensitive to the prediction residuals, as the covariances decrease. In the present case the final estimation, having smaller noise covariances, allows proportionally less error in model predictions. To achieve this tighter fit to the data, parameter values are estimated which are more extreme than those under larger noise statistics (see Appendix D).

4.5.2 Evaluation of Final Model Based on Statistical and Visual Analysis

Intake temperature predictions from the final model (eg., Figures 4-1 to 4-3) show qualitatively reasonable performance. The predictions frequently differ from the measurements by several degrees, but follow the data pattern fairly well.

However, model test results in Table 4-3 indicate that statistically the final model is unacceptable. The model fails the test on the S-value (Section 2.2). In only one data period is S found within $2\sigma_S$ of its expected value; in the other three periods, S is considerably below E[S]. The model also fails the whiteness test (Section 2.2). Significant autocorrelation of the residuals is observed, in all data periods. P(a) is frequently greater than 5, whereas an acceptable model should have all P(a) less than 5.

Based on least-squares performance measures, the final model also appears unsatisfactory. Both M (mean-square error of hourly predictions) and D (mean-square error of daily peak predictions) are undesirably high (greater than 10.0) in all four data periods.

The low S values are probably not due to erroneous noise statistics. The final noise estimates are so small that S, during the base period, is almost within 2 σ_S of its expected value. Further reduction is unrealistic, and probably cannot correct the large discrepancies observed for the test periods.

Failure to pass the statistical tests (on S and whiteness) indicates flaws in either the structural or probabilistic aspects of the model. The fundamental assumptions of FIML parameter estimation are that:

1. The proposed linear model structure is the true structure.
2. Model disturbances represent a white, Gaussian process.

If these assumptions are met, then FIML parameter estimates are optimal (Section 2.1). Peterson (1975) further demonstrates, with simulation experiments, that under these assumptions FIML estimation is a very accurate parameter estimation method. Thus, if the true model structure is known and linear, FIML parameter estimates will be close to the true estimates (on the average) and will pass the statistical tests. Not passing the tests suggests errors in model structure and/or probabilistic assumptions, prohibiting successful FIML estimation.

An alternate explanation is that the base period for estimation is abnormal or too short. The consistent performance improvement between the preliminary and final models (see Section 4.5.5.) suggests that the base period used here is adequate. However, evaluation of statistical performance for different base periods is not done, so the importance of this effect is not known. As further estimation experience with water quality models accumulates, a better rule-of-thumb for base period length may evolve.

4.5.3 Evaluation of Model Performance in Terms of Original Performance Criteria

The final model does not meet the accuracy criterion specified in the original model development problem (T > 90%). In its best data period (8/23-9/20), the final model yields T = 27%. Over all four data periods, the final model yields an average T = 17%. Thus, the model developed in this study should not be used for STF applications at present.

The final model does meet the other performance criteria, i.e., it is simple, and it performs real-time prediction using only existing sensors.

4.5.4 Comparison of Final Model with Results of Earlier Studies

Earlier efforts to model intake water temperatures at Salem Harbor Station are reported by Kenison and Galli (1975). Two types of peak-to-peak extrapolation models are reported (Section 3.1): a subjective model using human intuition to make predictions, and a multiple regression model. A comparison of model performance between past and present studies is presented in Table 4-4. (T is the only model performance measure reported by Kenison and Galli).

Based on Table 4-4, no model achieves the original accuracy criterion, $T \geq 90\%$. Subjective peak-to-peak prediction performs best, and multiple regression peak-to-peak prediction is second best. Both peak-to-peak extrapolation models perform better than the basin-type model. Possible explanations for these differences in performance are proposed below.

The results in Table 4-4 compare initial model development efforts for three model structures. It appears that, in the initial stages of model development, a subjective peak-to-peak model is most effective. The present modeling problem is well-suited for subjective peak-to-peak modeling, in the following ways:

- the system has a long time-constant relative to the desired prediction interval (ie., day-to-day changes in peak temperature are typically $1^{o} - 2^{o}F$)
- only one or two states must be predicted
- measurements from only one or two locations are used

TABLE 4-4

PAST AND PRESENT MODEL PERFORMANCE

Model	Evaluation Period	T
Kenison and Galli - Subjective	6/1 - 7/31/74	43%
Kenison and Galli - Multiple regression	6/1 - 7/31/74	34%
Present study	6/25 - 7/22/74	16%
- Basin-type	8/23 - 9/20/74 (best)	27%
	5/17 - 9/20/74 (overall)	17%

(Where T equals the percentage of daily peak intake temperature predictions within $\pm$ 1°F of observed.)

Under these conditions, much of the variation in peak intake temperatures may be explained by a simple, subjective, peak-to-peak model structure.

Since none of the models achieves the desired accuracy, one or more must be developed further. Although the peak-to-peak models yield initially high T values, further accuracy improvements for this model structure are not expected to be major. Ultimately, hourly temperature models are expected to yield maximum accuracy. Present peak-to-peak models capture the major factors influencing peak temperatures, but are likely to require detailed treatment of hourly processes to achieve improved accuracy.

It appears from table 4-4 that models for hydrothermal control problems similar to that addressed in this thesis may be more effectively developed from statistical concepts than from physical concepts. A statistical model can be algebraically much simpler than a physically-derived model of the same process. Whereas a physical model requires calculation of temperature within every discretized cell, a statistical model may eliminate all state variables except those to be controlled. The model comparison above suggests that by eliminating extraneous considerations, a simple statistical model may predict the controlled variable(s) more accurately than a physical model. Statistical models offer two additional advantages: First, parameter estimation costs are much less for simpler models; also model structure revision is easier, allowing faster evolution of the model. For these reasons, pursuit of a statistically-derived, hourly model appears to offer the greatest potential accuracy.

4.5.5 Comparison Of Final And Preliminary Models

Phase I of the estimation process produces preliminary parameter values, representing the best subjective estimates obtainable. Final parameter values are refined from the preliminary values, in phase II using global FIML estimation. Comparing the performance of the preliminary and final models indicates how much model performance is improved by global FIML parameter estimation.

Such a comparison shows that the final model performs slightly better than the preliminary model throughout the latter three (summer) data periods. Inspection of Table 4-3 shows for these periods:

Log-likehood: Final model is consistently better by a slight amount ($\Delta \xi = 50$).

S: Final model yields S consistently higher, and closer to E [S].

T: Final model is better for one period; models are equivalent for other two periods. T(2^o) and T(3^o) are consistently better for final model.

D: Final model is consistently better.

M: Final model is better for two periods, worse for one.

Whiteness: Final model is consistently better for P(0) and P(3); consistently worse for P(1) and P(2).

$\sigma_z^2(24|1)$: Final model is better.

The improvement in performance observed in the test periods is comparable to that achieved for the base period.

The late - spring period (5/17 - 6/13) is anomolous. For this period, the preliminary model is better than the final model by almost all measures. A likely explanation is that different processes dominate habor temperatures during the late-spring period, than during the summer period for which the final parameters are estimated. An important example is stratification, which is only partly established during the late spring period, but fully established during the summer periods. Because this period is anomolous, further comparison of final and preliminary models considers only the latter three data periods.

Though the final model generally yields better measures of performance than the preliminary model, the differences are often small. The performance of the final model is poor (see statistical evaluation); relative to the amount of improvement needed, the improvement achieved by FIML estimation is also small. In addition, the final model is not always superior to the preliminary model (for example, see the whiteness and T values). For these reasons the final model is considered only slightly better than the preliminary model.

The limited improvement in performance achieved by FIML estimation is probably due to two factors. First, the preliminary estimates are likely to be very good. These estimates incorporate extensive engineering experience, plus adjustments to fit the model to a 294-hour base period. Thus, the preliminary estimates are likely to perform fairly close to the optimum for this model structure.

Flaws in the model structure are the second factor likely to be limiting model improvement from FIML estimation. Structural flaws may restrict model performance to low levels, even at the optimum.

Previous analysis (Section 4.5.2) strongly suggests that structural flaws exist in the model, inhibiting significant model improvement via parameter estimation.

Given a model with structural flaws, the improved performance of the final model is an important result. It demonstrates that FIML estimation can yield improved parameter estimates, even in the presence of a structurally weak model. This robust character is essential for a practical parameter estimation tool, since few model development problems begin with an accurate model structure.

4.5.6 Structural Flaws In The Model

Several results indicate that structural errors exist in the model:

- $S \neq E[S]$
- $P(a) > 5$
- M and D>10
- Unrealistic final parameter values
- Limited model improvement achieved by FIML estimation

Structural weaknesses are most likely in the following areas of the present model:

- Formulation of net surface heat flux: These processes are not well understood, particularly on an hourly time scale. Recent experiments by Hecker and Nystrom (1975) indicate that the formulation used herein will underestimate surface heat loss, on the average. This partially explains the chronically high temperature predictions obtained from the preliminary model.

- Treatment of tidal flushing:

A better model of the open boundary condition is desirable, taking into account heat losses in Salem Sound.

- Discretization: The four cells in the present model are assumed well-mixed, though they actually are not. For example, concentrations of heat near the discharge (ie., the thermal plume) are averaged into the overall temperature of the inner cell. Hence on ebb tide, this heat is not all flushed out as it is in nature, leading to abnormally high temperature predictions. A finer discretization may be required.

Further effort refining the present model is not recommended. Rather, future model development effort should focus on hourly statistical models as recommended in Section 4.5.4.

4.5.7 Applicability of FIML Estimation

In the present model development problem, subjective model development yields large initial performance improvements. FIML estimation yields consistent (but small) improvement, in this initial iteration of model development. However, future refinement of model accuracy requires more detailed treatment of many factors, on an hourly time scale. FIML estimation becomes increasingly valuable in the latter iterations of model development, as structural complexity increases (and approaches the true structure).

In other modeling problems more complex than the present, subjective development yields smaller improvements. FIML estimation is proportionately more valuable for these modeling problems, where:

a. Several states are predicted simultaneoulsy, and it is desired to minimize the overall uncertainty.

b. Relatively frequent predictions (on the order of measurement frequency) are made, and it is desired to minimize the uncertainty over the whole time-stream.

c. The system has a relatively short time-constant, necessitating more detailed modeling of system behavior.

d. Point predictions in time and space are desired, rather than averages.

e. Several measurements are taken simultaneously, and it is desired to make optimal use of all information.

f. Long data records are to be processed for model development.

CHAPTER FIVE

SUMMARY AND CONCLUSIONS

5.1 Summary

The objectives of this study are:

1. To solve the model development problem: ie., develop a simple model of intake water temperatures at Salem Harbor Station that predicts the daily peak intake temperature within 1°F, 90% of the time.

2. To apply optimal filtering and maximum likelihood parameter estimation to a water quality model of a real system using field data. Evaluate the advantages of these techniques in this application.

No previous hydrothermal model is developed and evaluated in terms of a pre-specified accuracy criterion. Nor, is a water quality model previously developed for a real system using full-information maximum likelihood parameter estimation.

A short-term temperature forecasting (STF) system is proposed, to minimize the cost of meeting the discharge water temperature limit at Salem Harbor Electric Generating Station. The STF system requires accurate predictions of power plant intake water temperatures, to determine reduced-cost power generation schedules.

Tools of estimation theory are shown to be potentially useful for model development. Optimal filtering and maximum likelihood parameter estimation are methods for estimating the states and parameters, respectively, of an uncertain dynamic system. Filtering yields optimal (minimum uncertainty) state estimates by combining

information from a model and from measurements. Full-information maximum likelihood (FIML) parameter estimation uses the filtered state estimates to compute model likelihood. The maximum likelihood is found by searching alternate parameter values, using Powell's method for non-linear optimization.

Statistical and physically-derived model structures are considered for the model development problem. A simple two-basin, two-layer hydro-thermal model of Salem Harbor is developed. The model includes effects of power plant discharge, tidal flushing, stratification, surface heat flux, and wind advection of the plume, to yield hourly predictions of intake water temperatures. The model is transformed into state-space, white process form, to allow application of estimation tools. In state-space form, the model is linear (non-linear in the inputs) and time-varying, and has six state variables and one observation.

Thirty-three parameters are either poorly known or unknown, and are estimated from intake temperature data. Initial values are chosen based on engineering judgement and data in the literature. Following preliminary, subjective tuning (over a 294-hour period), FIML estimation is used to obtain globally optimal parameter estimates (over a 96-hour period). The resulting model's performance is tested for 106 days during late spring and summer of 1974. Quantitative and qualitative measures of performance are computed. The model and the FIML estimation method are evaluated from analysis of the test results, and from comparisons with earlier models.

5.2 Conclusions

1. The two-basin, two-layer model developed in this study is qualitatively correct, but fails statistical tests for acceptability.

2. The two-basin, two-layer model does not meet the accuracy criterion specified in the model development problem.

3. Simple peak-to-peak extrapolation models predict daily peak intake temperature more accurately than a simple hourly basin-type model.

4. Different processes dominate harbor temperatures during late-spring than during summer. In the two-basin, two layer model, different parameter values are required to model each period.

5. Structural inadequacies exist in the two-basin, two layer model, causing limited model performance. Possible improvements in model structure are discussed below.

6. Full-information maximum likelihood parameter estimation is useful for development of water quality models. In an application to a real system, using field data, this method:

    a. Estimates thirty-three unknown parameters from ninety-six data points.

    b. Improves parameter estimates from their best *a priori* values, despite flaws in the model structure.

7. Full-information maximum likelihood parameter estimation is most useful for development of water quality models where:

    a. Subjective model development is thoroughly exercised

    b. Several states are predicted simultaneously

    c. Relatively frequent predictions (on the order of measurement frequency) are made

    d. The system has a short time-constant

    e. Point predictions in time and space are made

    f. Several variables are measured

    g. Long data records are to be processed

5.3 Recommendations For Future Work

1. Future model development for hydrothermal control problems should use an hourly statistical model, rather than physically-derived structures. Statistical models offer:

   a. Faster development

   b. Potentially greater accuracy

   c. Lower cost

2. To improve the two-basin, two-layer model, the following changes are suggested:

   a. Revise the formulation for net surface heat flux. Consider a simpler formulation, with parameters estimated from a long period of hourly data.

   b. Revise the open boundary condition

   c. Use a finer discretization of Salem Harbor

3. Further evaluation of FIML estimation should be done:

   a. Compare model performance using FIML estimates from a 96-hour data base with performance using estimates from a longer data base.

   b. Compare performance using FIML estimates with performance of ordinary least squares estimates. Also compare estimation costs.

BIBLIOGRAPHY

Aoki, M. Introduction to Optimization Techniques: Fundamentals and Applications of Non-Linear Programming. MacMillan Co., New York, N.Y. (1971).

Army Corps of Engineers, Addition of Unit No. 5, Salem Harbor Electric Generating Station, Salem Massachusetts--Draft Environmental Statement. Department of the Army, New England Division, Corps of Engineers, Waltham, Mass. (March, 1975).

Atomic Energy Commission, Final Environmental Statement Related to the Proposed Seabrook Units 1 and 2. Docket nos. 50-443 and 50-444, U.S. Atomic Energy Commission, Washington, D.C. (Dec., 1974).

Baeyens, R. and B. Jacquet, "Applications of Identification Methods in Power Generation and Distribution", in Identification and System Parameter Estimation, Part II. (P. Eykhoff, ed.) North-Holland/American Elsevier, New York, N.Y. (1973).

Box, G.E.P. and G.M. Jenkins, Time Series Analysis: Forecasting and Control, Holden-Day, Inc., San Francisco, Calif. (1970).

Chesmore, A.P. et al. Investigations of the Effects of Electrical Power Generation on Marine Resources in Salem Harbor, Progress Report Nos. 1-11, 1/72 - 8/74. Div. of Marine Fisheries, Dept. of Natural Resources, Commonwealth of Mass. (January, 1972 - August, 1974).

Coastal Research Corporation, Airborne Thermal Imagery of Discharge Plume Dispersion. Coastal Research Corporation, Box 281, Lincoln, Mass. (Nov. 9, 1972) (Prepared for New England Electric System, Westboro, Mass.).

Commonwealth of Massachusetts, Water Resources Commission, Division of Water Pollution Control, "Rules and Regulations for the Establishment of Minimum Water Quality Standards and for the Protection of the Quality and Value of Water Resources". (May 2, 1974).

Crawford, J. Personal Communication. New England Power Service Co., Westboro, Mass.

Desalu, A.A. Dynamic Air Quality Estimation in a Stochastic Dispersive Atmosphere. Report No. ESL-R-542, Electronic Systems Laboratory, MIT, Cambridge, Mass. (April, 1974).

Docket No. MA0005096 , in re Salem Harbor Station Units #1 - 4 NPDES Permit Proceedings, Permits Branch, Environmental Protection Agency, Region 1, Boston, Mass.

Elwood, J. R., "Thermal Pollution Control In Massachusetts Coastal Waters", Massachusetts Water Resources Commission, Division of Water Pollution Control, Publication No. 6505 (16-400-12-72-CR) Boston, Mass. (Jan. 1973).

Environmental Protection Agency, "Steam Electric Power Generating Point Source Category", Federal Register, Vol. 39, Page 36186 (October 8, 1974).

Environmental Protection Agency, "Thermal Discharges", Federal Register, Vol. 39, Page 36176 (October 8, 1974).

Environmental Protection Agency, "National Pollutant Discharge Elimination System". Federal Register, Vol. 38, Page 13528 (May 22, 1973).

Fairbanks, R. B., W. S. Collings, and W. T. Sides, An Assessment of the Effects of Electrical Power Generation on Marine Resources in Cape Cod Canal. Division of Marine Fisheries, Dept. of Natural Resources, Commonwealth of Mass. (March 13, 1971).

"Federal Water Pollution Control Act Amendments of 1972", Public Law 92-500, 92nd Congress, S. 2770, October 18, 1972, Office of Public Affairs, U.S. Environmental Protection Agency, Washington, D.C., (1972).

Fletcher, R. and M. J. D. Powell. "A Rapidly Convergent Descent Method for Minimization". The Computer Journal, Vol. 6, No. 163, (1967).

Gustavsson, I. "Survey of Applications of Identification in Chemical and Physical Processes" in Identification and System Parameter Estimation, Part I. (P. Eykhoff, ed.) North-Holland/American Elsevier, New York, N.Y. (1973).

Hamon, R. W., L. L. Weiss, W. T. Wilson, "Insolation as an Empirical Function of Daily Sunshine Duration", Monthly Weather Review, Vol. 82, No. 6 (June, 1954).

Harleman, D. R. F., D. N. Brocard, and T. O. Najarian, A Predictive Model for Transient Temperature Distributions in Unsteady Flows. Ralph M. Parsons Laboratory for Water Resources and Hydrodynamics, MIT, Cambridge, Mass.; TR No. 175, (Nov., 1973).

Harleman, D. R. F. Transport Processes in Water Quality Control, Civil Engineering Dept., Mass. Institute of Technology, (1974).

Harleman, D. R. F. and K. D. Stolzenback, Engineering and Environmental Aspects of Heat Disposal from Power Generation. Dept. of Civil Engineering, MIT, Cambridge, Mass. (June, 1975).

Jirka, G. H., G. Abraham, and D. R. F. Harleman, An Assessment of Techniques for Hydrothermal Prediction, Ralph M. Parsons Laboratory for Water Resources and Hydrodynamics, MIT, Cambridge, Mass.; TR No. 203 (July, 1975).

Kenison, A. R. and K. G. Galli, Power Plant Cooling Water Temperature Prediction - Subjective Versus Computerized Analysis Techniques, Proceedings, 21st Annual Meeting of Institute of Environmental Sciences (held on 4/13-16/75).

Kinne, O. (Ed.), Marine Ecology, Vol. I, Part 2, Wiley-Interscience, London, England (1970).

Koivo, A. J. and G. R. Phillips, "Identification of Mathematical Models for DO and BOD Concentrations in Polluted Streams from Noise Corrupted Measurements", Water Resources Research, Vol. 7, No. 4 (August, 1971).

Koivo, A. J. and G. R. Phillips, "On Determination of BOD and Parameters in Polluted Stream Models from DO Measurements Only" Water Resources Research, Vol. 8, No. 2 (April, 1972).

Lee, E. S., and I. Hwang, "Stream Quality Modeling by Quasilinearization" Journal of the Water Pollution Control Federation, Vol. 43, No. 2 (Feb., 1971).

Maine Yankee Atomic Power Co., Maine Yankee Atomic Power Station Environmental Report, Supplement No. One, Vol. I. Wiscasset, Maine.

"Massachusetts Clean Waters Act", Environment Reporter, pp. 806: 0101-0112, Bureau of National Affairs, Inc. Washington, D.C. (1974).

Matthews, W., "Environmental Management", MIT course, Spring, 1975.

New England Electric System, Annual Report and Statistical Supplement for 1974. Westborough, Mass. (1974).

Peterson, D. W. and F. C. Schweppe, "Code for a General Purpose System Identifier and Evaluator (GPSIE)", IEEE Transactions on Automatic Control, Vol. AC-19, #6: 852-4 (Dec., 1974).

Peterson, D. W., Hypothesis, Estimation and Validation of Dynamic Social Models - Energy Demand Modeling, Ph. D. Thesis, Dept. of Electrical Engineering, MIT, Cambridge, Mass. (June, 1975).

Powell, M. J. D., "An Efficient Method for Finding the Minimum of a Function of Several Variables Without Calculating Derivatives", The Computer Journal, Vol. 7, No. 155, (1964).

Rault, A., "Identification Applications to Aeronautics", in Identification and System Parameter Estimation, Part I. (P. Eykhoff, ed.) North-Holland/American Elsevier, New York, N.Y. (1973).

Rose, D., "National Socio-Technological Problems and Responses", MIT course, Spring, 1975.

Ryan, P. J. and D. R. F. Harleman, An Analytical and Experimental Study of Transient Cooling Pond Behavior. Ralph M. Parsons Laboratory for Water Resources and Hydrodynamics, TR No. 161, MIT, Cambridge, Mass. (1973).

Schweppe, F. C., Uncertain Dynamic Systems. Prentice-Hall, Inc., Englewood Cliffs, N.J. (1973).

Shastry, J. S., L. T. Fan, and L. F. Erickson, "Non-Linear Parameter Estimation in Water Quality Modeling", Journal of the Environmental Engineering Division, American Society of Civil Engineers, (June, 1973).

Stengel, R. F., G. Luders, E. Ruber, J. B. Carr, The Evaluation of Thermal Discharge Effects on Aquatic Biological Communities, The Analytical Sciences Corporation, Reading, Mass. TR-650-1, (1/9/75).

Tsai, Y. Personal Communication, Stone and Webster Engineering Co., Boston, Mass.

TSP: Time Series Processor (Version 2.4), Technical Paper #12, Harvard Institute of Economic Research, Harvard University, Cambridge, Mass. (1974).

Ulanowicz, R. E., D. A. Flemer, D. R. Heinle, and C. D. Mobley, The A Posteriori Aspects of Estuarine Modeling ( ). Chesapeake Biological Laboratory, Natural Resources Institute, University of Maryland, Solomons, Maryland.

Water Resources Engineers, Inc., Second Progress Report: Investigation of Alternative Procedures to Estimate Ground Water Basin Parameters. Walnut Creek, Calif. (July, 1973).

Young, P. C., S. H. Shellswell, and C. L. Neethling, A Recursive Approach to Time-Series Analysis, Dept. of Engineering, University of Cambridge, England, CUED/B-Control/TR16 (1971).

Young, P. and P. Whitehead, A Recursive Approach to Time-Series Analysis for Multivariable Systems. Control Division, Dept. of Engineering, University of Cambridge, England (1974).

Young, P. and B. Beck. "The Modelling and Control of Water Quality in a River System", Automatica, (Sept., 1974).

Zangwill, W.I, "Minimizing a Function Without Calculating Derivatives", The Computer Journal, Vol. 10, No. 293, (1967).

Nystrom, J.B. and G.E. Hecker, "Experimental Evaluation of Water to Atmosphere Heat Transfer Equations", (presented at 1975 ASCE Annual Convention) Alden Research Laboratories, Holden, Mass. (1975).

Schrader, B.P., Once-Through Cooling at Salem Harbor Electric Generating Station: Short-term Temperature Forecasting, and Policy Aspects of a Temperature Standard, Environmental Engineer's Thesis, Department of Civil Engineering, MIT, Cambridge, Mass., (1976).

APPENDIX A

MODEL EQUATIONS FOR NET SURFACE HEAT FLUX

Except where otherwise noted, the following development of heat flux terms is taken from Harleman and Stolzenbach (1975). Where appropriate, their equations (for daily fluxes) are modified with unknown parameters, F_i, to produce hourly values. All fluxes are computed in units of BTU/ft^2-hour.

Harleman and Stolzenbach (1975) indicate that net surface heat flux is the sum of fluxes due to several heat exchange processes occurring at the water-air interface:

$$\text{Net Surface Heat Flux} = \phi_n = \phi_{sn} + \phi_{an} - \phi_{br} - (\phi_e + \phi_c) \qquad (1)$$

where ϕ_{sn} = net shortwave insolation

ϕ_{an} = net atmospheric radiation (longwave)

ϕ_{br} = longwave radiation from water surface

$\phi_e + \phi_c$ = evaporative and conductive heat flux

Net shortwave insolation is the product of several factors:

$$\phi_{sn} = \phi_{sc} \cdot f_1 \text{ (time-of-day)} \cdot f_2 \text{ (cloudiness)} \qquad (2)$$

where ϕ_{sc} = net daily clear-sky insolation

f_1 = proportion of total daily insolation occurring in a given hour

f_2 = radiation reduction factor due to cloudiness

These factors are computed as follows:

$$\phi_{sc} = [38.4 \sin (\frac{2\pi}{365} \cdot \text{Julian Day} + \frac{\pi}{2}) + 490] \cdot F_8 \quad (3)$$

where Julian Day = day number, consecutive from January 1

F_8 = bias adjustment parameter

Equation (3) fits the curve developed by Hamon et al (1954) for maximum total daily sunshine at 42°N latitude. The equation is modified by F_8 to correct potential bias in ϕ_n. A bias in ϕ_n is anticipated because equations originally developed for daily flux computations are being adapted for hourly computations (below).

$$f_1 = \begin{cases} .5 \sin [\frac{2\pi}{30} (t - 6)], & \text{for } 0600 < t < 2100 \\ 0 \quad , & \text{for } t < 0600 \text{ or } t > 2100 \end{cases} \quad (4)$$

where t = time-of-day (from 0001 to 2400).

$$f_2 = 1 - F_1(\frac{c - 1}{3}) \quad (5)$$

where c = cloudiness (ranging from 1 (clear) to 4 (very cloudy))

F_1 = maximum radiation reduction.

This equation is suggested by Harleman and Stolzenbach (1975) who use $f_2 = 1\text{-}65\ c^2$, with c varying from 0 to 1. The exponent is dropped here, to increase sensitivity to partial cloudiness.

Net atmospheric radiation is also the product of several factors:

$$\phi_{an} = F_2 \cdot 10^{-15}(460 + T_{air})^6 [1 + F_3 (\frac{c - 1}{3})^2] \quad (6)$$

where T_{air} = air temperature (°F)

F_2 = net atmospheric radiation parameter

F_3 = maximum radiation increase due to cloudiness

Note that the first factor in Eq. (6) represents net clear-sky atmospheric radiation. The second factor accounts for increased atmospheric radiation with increased cloudiness.

The longwave back-radiation from the water is modeled by:

$$\phi_{br} = F_7 \times 10^{-9}[460 + (F_6 \cdot T_S)]^4 \qquad (7)$$

where T_S = temperature of surface layer (°F)

F_7 = back-radiation parameter

F_6 = back-radiation temperature sensitivity parameter.

Since T_S varies between basins, ϕ_{br} is computed separately for each basin.

The evaporative and conductive heat flux is modeled by:

$$\phi_e + \phi_c = F_5 \cdot WS\ [(e_s - e_{air}) + .255\ (T_S - T_{air})] \qquad (8)$$

where WS = wind speed

e_s = vapor pressure at water surface

e_{air} = vapor pressure of air

F_5 = evaporative-conductive heat flux parameter.

The saturated vapor pressure, e_s, is obtained from Harleman et al (1973):

$$e_s = -2.4875 + .2907\ T_S - .00445\ T_S^2 + .0000663\ T_S^3 \qquad (9)$$

By substituting in Eq. (9) the dewpoint temperature for T_S, one may also obtain e_{air}. Evaporative and conductive heat flux must be computed separately for each basin.

In order to apply optimal filtering, the heat flux equations must be linear in T_S. Non-linearities exist in the above formulations of ϕ_{br} and $\phi_e + \phi_c$. These are linearized about the filtered state estimate, $\hat{T}_S(n|n)$, using a first-order Taylor series expansion:

$$f(T_S(n)) \approx f(\hat{T}_S(n|n)) + f'(\hat{T}_S(n|n)) \cdot [T_S(n) - \hat{T}_S(n|n)]$$

For $f = \phi_{br}$, the derivative is:

$$\phi'_{br} = F_4 \times 10^{-9}[460 + (F_6 \cdot \hat{T}_S(n|n))]^3$$

where F_4 = linearized back-radiation parameter.

For $f = \phi_e + \phi_c$, the derivative is:

$$(\phi_e + \phi_c)' = F_5(WS)[.5457 - .0089\ (\hat{T}_S(n|n)) + .0001989\ (\hat{T}_S(n|n))^2].$$

APPENDIX B

SOURCES OF DATA

I. Data Used To Run Hourly Two-Basin, Two-Layer Model
(For Period 17 May 1974 to 20 September 1974)

Data	Frequency/Measurement Point	Source
Intake Temperature	Hourly instantaneous measurements. Floating sensor 2 ft. below water surface, 30 ft. offshore of unit #3.	New England Power Company (NEPCO) computerized environmental data bank.
Discharge Temperature	Hourly instantaneous measurements hourly. Floatting sensor 2 ft. below surface, in discharge canal 200 ft. from mouth.	NEPCO computerized environmental data bank.
Wind Speed and Wind Direction	Hourly instantaneous measurements. Sensor at 100 ft. elevation, atop Breaker House at Salem Harbor Station.	NEPCO computerized environmental data bank.
Condensor Flow Rate	Continuous records for each unit showing when circulating water pumps are on or off.	Mechanical log of each unit at Salem Harbor Station.
Cloudiness	Three-hourly measurements. Subjective assessment by station personnel.	Environmental log of Salem Harbor Station.
Air Temperature	Hourly instantaneous measurements. Sensor at 20 ft. elevation, atop Gate House at Station.	NEPCO computerized environmental data bank.
Dewpoint Temperature	Three-hourly instantaneous measurements at Logan Airport, Boston.	"Local Climatological Data, Logan International Airport", National Oceanic and Atmospheric Administration.

Data	Frequency/Measurement Point	Source
Tide Level	Predicted time and height of high and low tides (corrected to Salem, Ma.).	"Times and Heights of High and Low Waters, Boston, MA, 1974,", National Oceanic and Atmospheric Administration
Temperature of Salem Sound	Bi-weekly instantaneous measurements at location #5 of Chesmore et al (1972-1975).	Chesmore et al (1972-1975).

II. Other Data Used In Model Development

Infra-red Overflights	Reported in Chesmore et al (1972-1975).
Boat Surveys of Temperature	Reported in Chesmore et al (1972-1975)
Bathythermograph Surveys	Reported in Chesmore et al (1972-1975). Additional data obtained from B. Ketschke Cat Cove Marine Laboratory, Salem, MA. August, 1972 surveys of Salem Sound by R/V "Ferrel" (National Oceanic and Atmospheric Administration-unpublished).
Continuous Harbor Temperatures	Locations "C" and "D" maintained and reported by Chesmore et al (1972-1975). Hourly data obtained from B. Ketschke (as above).
Water Velocity	Reported in Chesmore et al (1972-1975).
Synoptic Studies	Interim Report: Salem Hydrothermal Survey Raytheon Environmental Research Laboratory, (August, 1972). (Done for NEPCO.)
Electric Generation Load	Hourly instantaneous measurements for each unit at Salem Harbor Station. See electrical log of each unit.

APPENDIX C

USING OPTIMAL FILTERING TO ESTIMATE UNMEASURED INITIAL CONDITIONS

To run the proposed model for real-time STF predictions, initial conditions $\underline{\hat{x}}(0)$ must be estimated. Data on harbor temperature (from buoy recorders, boat surveys, etc.) is infrequently collected, and thus is not likely to be available when a model run is desired. The only data available in real time are measurements of plant intake temperatures (z(n)).

Without direct measurements of $\underline{\hat{x}}$ (0), one approach is to subjectively estimate the harbor temperatures $\underline{\hat{x}}(0)$ from z(0). Such an estimate is very uncertain, especially since the six elements of $\underline{\hat{x}}(0)$ are estimated from only one measured value. An alternative approach is to estimate $\underline{\hat{x}}(0)$ from the previous 24 hours of data, using optimal filtering.

The approach begins at n = -24 with an uncertain estimate, $\underline{\hat{x}}(-24)$. The model is run forward from n = -24 to n = 0 and combined with data z(n), to obtain filtered estimates $\underline{\hat{x}}(n|n)$. The initial conditions for the STF prediction are thus:

$$\underline{\hat{x}}(0) = \hat{x}(0|n = -24 \text{ to } 0).$$

Figure C-1 presents an example of this approach, showing filtering of initial conditions, followed by unfiltered prediction. Experiments with this approach indicate that 24 measurements are sufficient to minimize the uncertainty in $\hat{x}(0|n)$.

FIGURE C-1

USING OPTIMAL FILTERING TO INITIALIZE STF PREDICTIONS

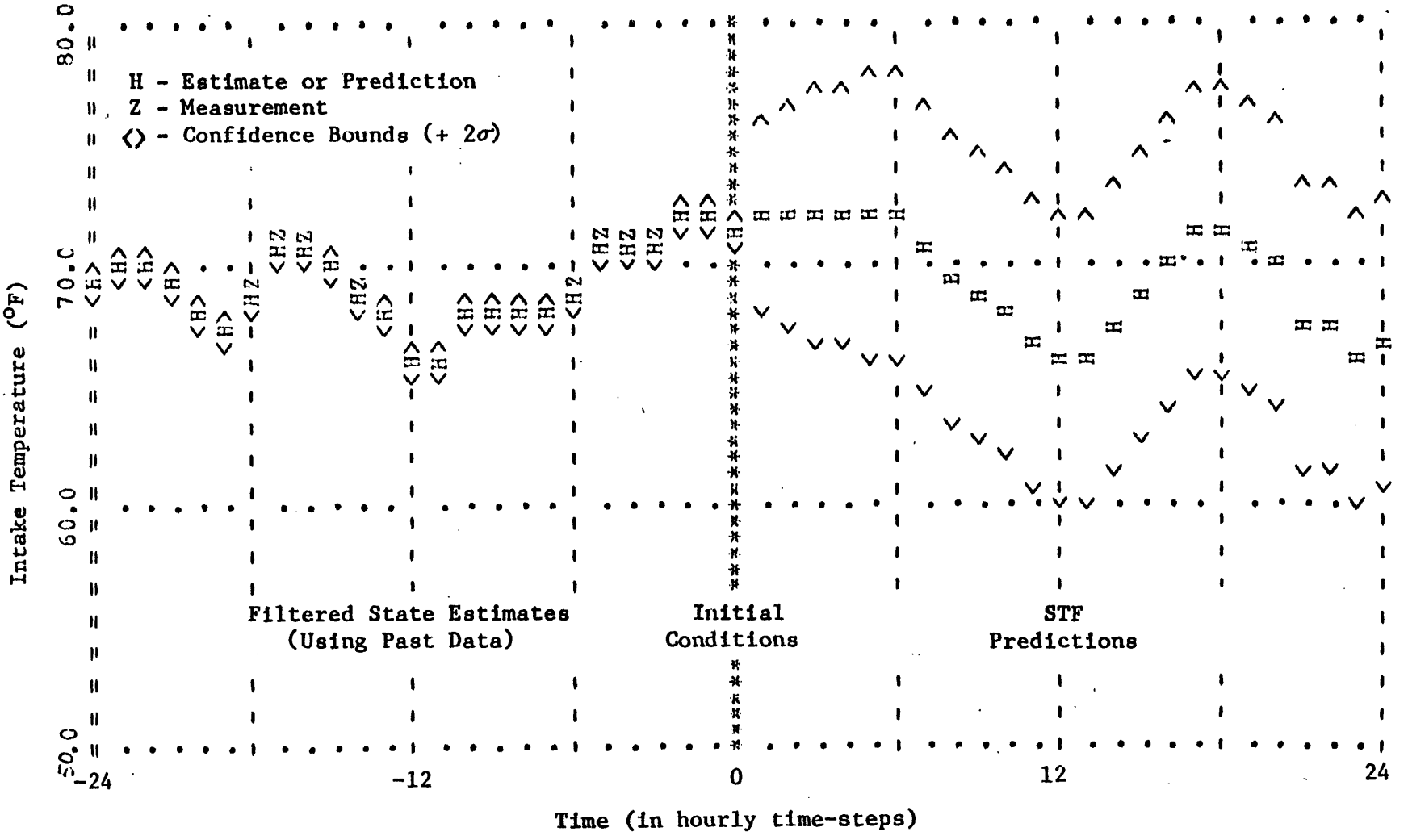

Appendix D

APPENDUM - IMPROVEMENT IN FINAL MODEL BY REDUCING MODEL NOISE (Q)

Following completion of this report, an additional computer run was done testing the optimality of the final noise statistics (σ_i). Tests (CF. Chapter Four) show that <u>increasing</u> σ_i <u>decreases</u> model performance as measured by S, the sum-of-squares of measurement residuals. The addition analysis just completed shows that further reducing σ_i below their "final" values <u>improves</u> model performance (see Table D-1). The S-statistic is very near its expected value, and the log-likelihood is also increased.

Thus, the noise statistics in Table D-1 are more nearly optimum than those in the "final" model presented in Chapter Four. At these revised noise levels, the optimum structural parameters may also be different (and <u>perhaps</u> more realistic) than the "final" model; however, a FIML estimate for new parameter values is not done.

TABLE D-1

IMPROVEMENT IN FINAL MODEL BY REDUCING MODEL NOISE (Q)

PARAMETER	FINAL MODEL	MODIFIED FINAL MODEL
σ^2_{S1}	3.	1.
σ^2_{B1}	2.	1.
σ^2_{S2}	1.5	1.
σ^2_{B2}	2.	1.5
σ^2_{Z}	.04	.04
Log-Likelihood	-87.0	-76.9
S	40.4	66.6
E [S]	63.	63.
σ_S	11.2	11.2